ICMSM 2024

3rd International Conference on Materials Science and Manufacturing

Editor:
Prof. Dr. Uğur KÖKLÜ

PROCEEDINGS

ISBN: 978-625-95311-6-8

15-16 November | 2024 | Turkey

url: https://matsciman.com

3RD INTERNATIONAL CONFERENCE ON MATERIALS SCIENCE AND MANUFACTURING (ICMSM 2024)
NOVEMBER 15-16, 2024

3. ULUSLARARASI MALZEME BİLİMİ VE İMALAT KONFERANSI (ICMSM 2024)
15-16 KASIM 2024

PROCEEDING E-BOOK/ BİLDİRİLER KİTABI

KARAMAN/TÜRKİYE

28.11.2024

ISBN: 978-625-95311-6-8

ICMSM 2024
3rd International Conference on Materials Science and Manufacturing

November 15-16, 2024

Online-Live

https://matsciman.com

Kasım, 2024/ November, 2024

ICMSM 2024

3rd International Conference on Materials Science and Manufacturing

3rd International Conference on Materials Science and Manufacturing (ICMSM 2024), will be held in Turkey during November 15-16, 2024 in online VIRTUAL format.

Conference Topics

- Additive manufacturing
- Biomaterals
- Casting
- Coating
- Composite materials
- Functional materials
- Forming
- Joining
- Labeling and painting
- Manufacturing
- Materials properties
- Materials science and engineering
- Machining
- Mechatronics
- Moulding
- Nano-materials
- New materials
- Shaping processes
- Surface treatment
- Smart materials
- Polymers
- Powder metallurgy
- Production
- Rapid prototyping
- Welding

Important Dates

Abstract Submission Deadline	October 15, 2024
Full Paper Submission Deadline	November 1, 2024
Registration Deadline	November 10, 2024
Conference Date	November 10, 2024

Language: Turkish and English

Conference Website
https://matsciman.com

ASES
ACADEMY OF SCIENTIFIC AND EDUCATIONAL STUDIES

General Information

Genel Bilgi

ICMSM 2024

3rd International Conference on Materials Science and Manufacturing
November 15-16, 2024
Online-Live
https://matsciman.com

Zoom Meeting Information

Please click on the zoom link provided for each session below or the link located in the each session on the program to attend the session of your choice. The Zoom application is free and no need to create an account. Any session can be joined without a password. Meeting passcode will be encrypted and included in the invite link to allow participants to join with just one click without having to enter the passcode. Speakers must be connected to the session 10 minutes before the presentation time.

Technical Information

- Make sure your computer has a microphone and is working.
- You should be able to use screen sharing feature in Zoom.
- Attendance certificates will be sent to you as PDF at the end of the congress.
- Moderator is responsible for the presentation and scientific discussion (question-answer) section of the session.
- Before you login to Zoom please indicate your name surname

exp. NAME SURNAME

Zoom Toplantı Bilgileri

İstediğiniz oturuma katılmak için lütfen aşağıda her oturum için verilen Zoom bağlantısına veya programdaki her oturumda yer alan bağlantıya tıklayın. Zoom uygulaması ücretsizdir ve hesap oluşturmanıza gerek yoktur. Herhangi bir oturuma şifre gerekmeden katılabilirsiniz. Toplantı şifresi şifrelenecek ve katılımcıların şifreyi girmeye gerek kalmadan tek tıklamayla toplantıya katılmasına olanak sağlamak için davet bağlantısına eklenecek. Konuşmacıların sunum saatinden 10 dakika önce oturuma bağlanması gerekmektedir. Tüm kongre katılımcıları canlı bağlanarak tüm oturumları dinleyebilir.

Teknik Bilgiler

- Bilgisayarınızda mikrofon olduğuna ve çalıştığına emin olun.
- Zoom'da ekran paylaşma özelliğine kullanabilmelisiniz.
- Katılım belgeleri kongre sonunda tarafınıza PDF olarak gönderilecektir.
- Moderatör – oturumdaki sunum ve bilimsel tartışma (soru-cevap) kısmından sorumludur.
- Zoom'a giriş yapmadan önce lütfen adınızı soyadınızı belirtiniz. Örnek: AD SOYAD

Communication

İletişim

Principal Contact
E-mail: kongre@matsciman.com
Web page: https://matsciman.com

ICMSM 2024

3rd International Conference on Materials Science and Manufacturing
November 15-16, 2024
Online-Live
https://matsciman.com

Moderating a Session

We appreciate all of the moderators' contributions to the conference. The moderators are expected to assist us in the smooth functioning of the conference.

- ❖ Please keep in mind that each presenter has a total of 20 minutes. It's important to have perfect timing.
- ❖ The moderator decides whether to take questions from the audience: at the end of each presentation or at the end of the session.
- ❖ Please remind attendees to send their questions and comments to the Zoom chat.
- ❖ Finally, if any of the presenters in your session does not participate and present her/his paper, please notify us by sending an email to kongre@matsciman.com.

Presentation Information

Each presentation has a **total time limit of 20 minutes**: 15 minutes for the presentation + 5 minutes for questions & answers. The moderator has the authority to rearrange the presentation order in the session. Please arrive at least 5 minutes prior to the start of your session and turn on your camera during your presentation. Please keep in mind that each presenter is required to remain for the duration of the session.

ICMSM 2024

3rd International Conference on Materials Science and Manufacturing

November 15-16, 2024

Online-Live

https://matsciman.com

Committees

Komiteler

Organizing Committee

- Aamer Sharif, Ph.D, Cecos University of IT and Emerging Science, Pakistan.
- Daniel Chuchala, Ph.D, Gdansk University of Technology Poland.
- Ekrem Oezkaya, Ph.D, Institute of Machining Technology, TU Dortmund, Germany.
- Eva Schmidova, Ph.D, University of Pardubice, Czech Republic.
- Fuat Kara, Ph.D, Düzce University, Türkiye.
- Gururaj Bolar, Ph.D, Manipal Academy of Higher Education, India.
- Khaled Giasin, Ph.D, University of Portsmouth, United Kingdom.
- Muhammad Faisal, PhD. Allama Iqbal Open University, Pakistan
- Uğur Köklü, Ph.D, Karamanoğlu Mehmetbey University, Turkey (Conference Chairman)

Science Committee

- A.Tamilarasan, PhD. Er.Perumal Manimekalai Engineering College, India.
- Engin Kocaman, PhD. Zonguldak Bulent Ecevit University, Turkey.
- Erkin Akdoğan, PhD, Karamanoğlu Mehmetbey University, Turkey.
- Grzegorz M. Królczyk, PhD, Opole University of Technology, Poland.
- Hüsnü Gerengi, PhD, Duzce University, Turkey.
- Ionut Cristian SCURTU, PhD. Eng., Naval Academy Constanta Romania
- Levent Urtekin, PhD, Kırşehir Ahi Evran University, Turkey.
- LokeshK Sri Ramamurth, PhD, Srinivas Institute of Technology, India.
- Mahmoud Khedr, PhD, Benha University, Egypt.
- Mitsuo Niinomi, PhD, Tohoku University, Japan.
- Mohamed A. Eltaher, PhD. King Abdulaziz University, Saudi Arabia.
- Muhammad Faisal, PhD. Allama Iqbal Open University, Pakistan
- Muhammad Pervej Jahan, PhD. Miami University, United States
- Murat Sarıkaya, PhD, Sinop University, Turkey.
- Mustafa Kuntoğlu, PhD, Selçuk University, Turkey.
- Oğuz Koçar, PhD. Zonguldak Bulent Ecevit University, Turkey.
- Shujian Li, PhD, Hunan University of Science and Technology, China.
- Şakir Yazman, PhD, Selçuk University, Turkey.

*Listed alphabetical order by name

From the President of the Conference,

Greetings to all participants,

It is a great pleasure for me to welcome you to the 3rd International Conference on Materials Science and Manufacturing (ICMSM) 2024 Conference.

We hope that this conference will create a friendly occasion for all to share perspectives and research findings from a wide variety of all engineering. We also dearly value possible friendships and partnerships made and insights gained at the conference and hope they will go beyond your participation in the conference, leading to better understanding and appreciation of our profession from an international stance.

With very best wishes,

Prof. Dr. Uğur KÖKLÜ

President of ICMSM 2024

Açılış Konuşması

Değerli katılımcılar Uluslararası Malzeme Bilimi ve İmalat konferans başkanı olarak sizleri en kalbi duygularımla selamlıyorum ve konferansımıza hoş geldiniz diyorum. Değerli katılımcılar davetimizi dikkate alarak Uluslararası Malzeme Bilimi ve İmalat Konferansına bildiri ile katılım sağladığınız için çok teşekkür ederiz. Uluslararası Malzeme Bilimi ve İmalat Konferansı çevrimiçi olarak gerçekleştirilecektir. Konferans, malzeme bilimi ve imalat alanındaki teknolojik gelişmeleri ve araştırma sonuçlarını sunmak ve paylaşmak için uluslararası bir platform görevi görecektir. Sanal ortamda dahi olsa sizleri ağırlamaktan ve bilgi paylaşımından dolayı çok mutlu oluyoruz. Umut ediyoruz ki sizlerle verimli ve unutulmaz bir konferans yaşayacağız. Konferansta toplam 9 bildiri sunulacaktır. Türkiye, Hırvatistan, İran, Malezya ve Hindistan'dan bilim insanlarının yer aldığı bildiriler sunulacaktır. Konferansımızda hem endüstriden hem de akademik camiadan bildiriler bulunmaktadır. Umut ediyorum ki arzulanan Üniversite ile endüstri bir araya gelerek çok başarılı çalışmalar yapılacaktır. Konferansta 2 oturum olacaktır. Bir sonraki konferansta görüşmek temennisiyle

Konferansımıza katıldığınız için tekrar teşekkür ederim.

Saygılarımla

Programme

Program

Friday, November 15, 2024 Time zone in Turkey (UTC+3)	**15 Kasım Cuma** 2024
Meeting ID: 269 738 6033 Password: 10abcd https://us06web.zoom.us/j/2697386033?pwd=wuIbEjghKmw0zfX8WafhkEKEzN9A8a.1&omn=88436760057 Click to connect/bağlanmak için tıklayınız	
09:00-09:20 AM	**Invited Speaker** Assoc. Prof. Ts. Dr. Noor Najmi Bonnia Universiti Teknologi MARA Shah Alam, Malaysia Optimizing Reaction Time in Modified Hummers Method for Synthesis of Graphene Oxide (GO) from waste tire
Session 1	**(09:20-10:40 AM)** **Session Chair: Dr. Sezer Morkavuk**
09:20-09:40 AM	Determination of Optimum Heat Treatment Parameters for Parts Produced by Forging Method Using Aw-4032 Quality Aluminum Raw Material Mert Karaman, *Ömer Batuhan Özkan,* Gizem Kocaman, Alper Kocakurt, Funda Gül Koç, Ersoy Erişir
09:40-10:00 AM	Topology Optimization of Gears for Additive Manufacturing Incorporating Static and Dynamic Performance Considerations Sepehr Pourrokni Salehan, *Hossein Soroush*, Saeed Khodaygan
10:00-10:20 AM	Investigation of Resistive Switching properties of Transition metal oxide-based nanostructure for flexible electronics Adiba Adiba, Tufail Ahmad
10:20-10:40 AM	3 Boyutlu Sterotigrafi Yazıcılarda Kullanılan Reçinenin Katkı Malzemeleri ile Geliştirilerek Düşük Basınçlı Plastik Enjeksiyon Cihazlarında Prototip Ürün Kalıbı Üretimine Uygun Dayanımda Kullanılabilecek Bir Reçinenin Araştırılması ve Uygulanması *Emre ÇİFTÇİ*, Efe Renç ELDENER
10:40 AM-02:00 PM Break	

Session 2	**(02:00-04:20 PM)** **Session Chair: Dr. Mehmet ŞAHBAZ**
02:00-02:20 PM	Spalatocrete – bio-composite made with spanish broom Sandra JURADIN, *Marijo FRANIĆ*
02:20-02:40 PM	The Utilization of 3DP in Miswak Holder Fabrication *Sharuddin BinMohd Dahuri*, Nor Hakimah Binti Ahmad Subri, Aliff Bin AB Tahir, Abu Harfiz Bin Hassan
02:40-03:00 PM	Photothermal Antibacterial Activity of Pani/Fly Ash Composite *Duygu YANARDAĞ KOLA*, Abdurrahman MUSTAFA, Ahmed ALSARORI, Gülcihan GÜZEL KAYA
03:00-03:20 PM	The influence of sinusoidal milling on surface quality of CFRP Sezer MORKAVUK, Uğur KÖKLÜ, Fatih Aktaş
03:20 PM Break	

PROCEEDINGS / BİLDİRİLER

FULL TEXT PRESENTATION / TAM METİN SUNUMLAR

TOPOLOGY OPTIMIZATION OF GEARS FOR ADDITIVE MANUFACTURING INCORPORATING STATIC AND DYNAMIC PERFORMANCE CONSIDERATIONS

Sepehr Pourrokni Salehan[1], Hossein Soroush[2], Saeed Khodaygan*[3]

[1]Department of Mechanical Engineering, Sharif University of Technology, Tehran, Iran, sepehrps@yahoo.com
[2]Department of Mechanical Engineering, Sharif University of Technology, Tehran, Iran, hossien.soroush@gmail.com
[3]Department of Mechanical Engineering, Sharif University of Technology, Tehran, Iran, khodaygan@sharif.edu

Abstract

Gears are crucial components in power transmission systems, and they transmit motion with the desired speed ratio between two shafts. In recent years, reducing the weight of gears has gained substantial attention across various industries due to its astounding advantages, such as enhanced energy efficiency and reduced dynamic loads. Furthermore, the ability of additive manufacturing (AM) to produce complex geometries allows for the optimal design of the gear body structure. This research presents a novel approach to reducing the gear's weight using topology optimization and design for AM methods. For this purpose, a spur gear made of 1023 steel has been studied as a case study. First, topology optimization is performed by considering the static loading conditions on the gear. To reduce the optimization process time, the critical section of the gear, where the keyway is located, is analyzed. In the next step, the optimized geometry for the gear body structure is redesigned to improve the manufacturability and reduce manufacturing time and cost. Then, the optimized geometry for the critical section is applied to the entire gear. The results indicate a reduction in gear weight by approximately 34% without significant changes in the induced stress on the gear tooth. Next, gear meshing stiffness is investigated to ensure the gear dynamic performance. Three models are studied: non-optimized spur gear (NOSG), topology-optimized spur gear (TOSG), and bottom-filled-optimized spur gear (BFOSG). Meshing stiffness value is estimated for each model using an analytical approach. The TOSG model demonstrates a 24% weight reduction and 58% stiffness reduction compared to the NOSG, which is remarkable and could significantly affect the gear's dynamic performance. On the other hand, the weight of the BFOSG is 83% of the NOSG, and its stiffness is about 88% of the NOSG model. Therefore, although the weight of the BFOSG model is slightly higher than the TOSG, its 46% higher meshing stiffness ensures the enhanced dynamic performance of the gear.

***Keywords*:** Gears, Topology optimization, Additive manufacturing (AM), Meshing stiffness

1. Introduction

AM is one of the most widely used manufacturing processes and has gained significant attention in the last two decades. In the AM procedure, samples are generated by adding layers of materials sequentially. This technology is utilized in medicine, education, architecture, and entertainment [1]. The AM market value was $8.35 billion in 2019 and is expected to reach $23.75 billion by 2027 with a growth rate of 14.4% [2]. The difference

between AM technologies lies in the material(s) used, how layers are created, and how they connect. These aspects determine the productivity and accuracy of the final products, as well as their mechanical properties [3].

AM is extensively used in the design and manufacturing of gears. Various studies investigated the design approaches and mechanical properties of additively manufactured gears [4-6]. Luszczek [4] reviewed the various AM techniques application in gears manufacturing. The results indicated that although AM can remarkably reduce the time and cost of gear production, there are main concerns about achieving the desired dimensional accuracy and surface finish, especially for 3D-printed gears made of polymers. He suggested that additively manufactured gears often need post-processing treatments to meet the wear resistance and fatigue lifetime requirements. Gupta [7] investigated the advancement in the AM industry for constructing gears using metals and plastics. He concluded that each 3D printing process has advantages for creating of complex geometries, manufacturing flexibility, and rapid prototyping. However, there is a need for further research in this era to resolve vibration, noise, and wear resistance problems. The parameters of AM can significantly affect the mechanical, dynamic, and thermal properties of the gear. For example, infill percentage affects the failure mechanism and lifetime of polymer additively manufactured gears. The proposed research showed that the infill percentage had a marked effect on the explored parameters for samples with less than 60% infill volume [8]. Besides these challenges, additively manufactured gear vibration and noise are among the most critical aspects considered for research. Yang et al. [9] studied the parameter optimization of a 3D printed aluminum gear to reduce the vibration in the gear. They optimized the holes configuration in the gear's body that were designed to reduce the gear's weight. The results showed a significant noise reduction according to the finite element simulation of three-floor gears. 3D-printed gear bearing vibrational behavior was explored by Moldovan [10]. The obtained results showed significant vibration in the gear which caused by manufacturing errors and gear's elastic deformation.

Topology optimization is a usual method used in the design stage to reduce the product weight and improve its performance. Design for additive manufacturing (DfAM) also employs topology optimization to create parts with maximum performance efficiency and minimum material usage. Brackett et al. [11] proposed a finite element-based topology optimization model that changes the size of tetrahedral cells of a lattice structure based on the stress magnitudes. They concluded that the presented model is effective since it does not need any iterative optimization method for varying the cell size and can be used for the topology optimization of AM species. Variable-density cellular uses for topology optimization of lattice structures. This approach is based on the homogenization that determines the lattice structure modules of elasticity according to their relative density. However, this method can be used only for homogeneous lattice structures [12]. Tyflopoulos et al. [13] studied the topology optimization for AM brake calipers using the solid isotropic material with penalization. The findings of their study revealed that the brake caliper's weight was reduced by approximately 40% after a redesigned stage of the optimized geometry.

According to the topology optimization advantages aligned with AM ability to create complicated geometries, this optimization approach can be implemented on gears DfAM. Becergen et al. [14] provided a novel framework to reduce the weight of the additively manufactured gears. They used mathematical methods to optimize the weight distribution in the inner body of the gears. The results indicated a 60% reduction in the gear's weight and a 49 MPa von Mises stress reduction obtained from the optimized structure. Patel et al. [15] optimized the gears of a continuously variable transmission (CVT) system. They used finite element analysis to evaluate the stress and deformation in gears. They concluded that the weight of the two studied gears was reduced by 5.2% and 12.5% without any significant

changes in the stress and deformation. Ramadani et al. [16] proposed a novel method to reduce the gear's weight and vibration by using topology optimization and finite element analysis. Their outcomes showed that the topology-optimzed gear had a lower noise level than the solid gear according to the sound signal measurements. Additionally, the results indicated that the topology-optimized gear noise can be further reduced when the polymer fills the cavities in the topology-optimized gear.

In summary, it is critical to consider the dynamic performance considerations for 3D-printed gears to ensure proper performance and minimize vibration and noise. This study investigates the static and dynamic performance of topology-optimized gears. For this purpose, meshing stiffness was used to evaluate the gear's dynamic performance. First, the topology optimization process has been done on the critical section of the gear using finite element analysis to reduce the gear's weight. İn the next step, the optimized geometry was redesigned to improve the manufacturability of the gears. Static carry loading was studied by considering the NOSG and TOSG models. Finally, three models were considered, and their meshing stiffness was compared to examine the dynamic performance of the desired gears. The BFOSG model presented the best results considering the meshing stiffness value and gear weight reduction.

2. Material and Methods

The topology optimization of the gear for AM by considering static and dynamic considerations involves seven steps illustrated in Figure 1. The optimization procedure starts with identifying the critical section in the gear. The critical section is a section of the gear with the highest stress value and stress concentration. In this research, the critical section was considered the area that contains the keyway location. In the next step, we performed the topology optimization on the selected critical section of the gear. The topology optimization details are discussed in section 2.1. Next, the obtained topology-optimized geometry was redesigned. This stage aims to simplify the gear's geometry. Although the AM has a noticeable ability to produce complex geometries, the initially obtained optimized geometry might has many voids that can affect the in-service lifetime of the gear negatively, leading to catastrophic failure and increasing the manufacturing time and cost. Furthermore, the finite element simulation of the initial model was not feasible due to the meshing issues. Therefore, the gear's geometry was redesigned to resolve these challenges (See section 2.2). In the fourth step, the redesigned model for the critical section was applied to the entire gear's body.

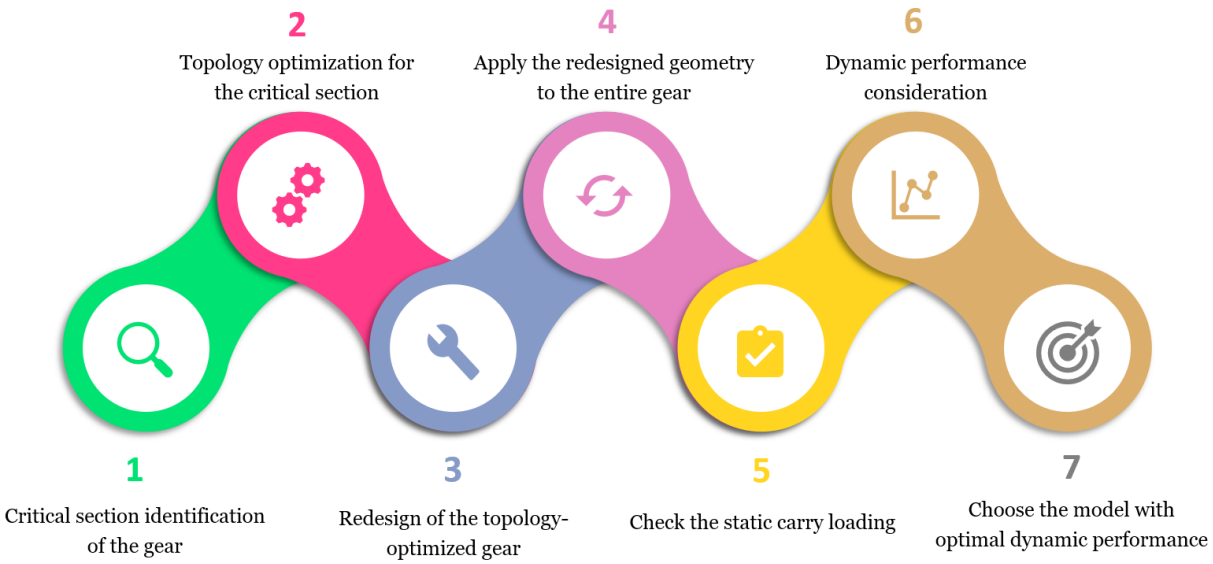

Figure. 1. The proposed roadmap for the topology optimization of the gear for AM

After obtaining the final geometry for the gear, its static carry loading was evaluated. For this purpose, a specific torsion was applied to the gear and the stress distribution was estimated in the gear's body. İf the maximum stress on the gear exceeds the allowable stress value, steps 1 to 4 must be repeated until the gear satisfies the static carry loading test. In the following step, the dynamic behavior of the gear was investigated. Exploring the gear's dynamic behavior is critical since it can notably affect the vibration and noise in the transmission system. According to the widespread application of gears in various industries, the manufacturing of gears with high rotational speed capability is rising recently. Therefore, studying the dynamic and vibration behavior in the gears gained significant attention. One of the most famous and usual ways to analyze the dynamic performance in gears is to determine the meshing stiffness. Meshing stiffness is caused due to the gear's teeth bending during the power transmission stage. There are different approaches to calculate the meshing stiffness in the gears. Analytical, finite element and experimental methods can be used for estimating the meshing stiffness. İn the presented research, an analytical method was used to calculate the meshing stiffness (See section 2.3 for details).

2.1 Topology Optimization Process

The studied gear in this research was a spur gear with the detailed specification presented in Table 1. First, the gear was modeled in Solidworks software. Figure 2.a shows the isometric view of the studied spur gear. As mentioned before, the critical section of the gear must be selected for the topology optimization. The critical section of the gear is shown in the Figure 2.b. Performing the topology optimization can change the model's geometry completetly. However, it is essential that the geometry of the gear's teeths have their initial shape for ensuring the gear meshing. Therefore, a 2 mm thick section was removed from the outer surface of the gear to ensure that the shape and geometry of this area remains unchanged (Figure 4). The 2 mm thick section was not considered in the topology optimization process.

Table 1 Characteristics of the studied gear.

Gear Specifications	Details
Module (mm)	10
Number of teeth	18
Material	1023 steel
Poisson's ratio	0.3

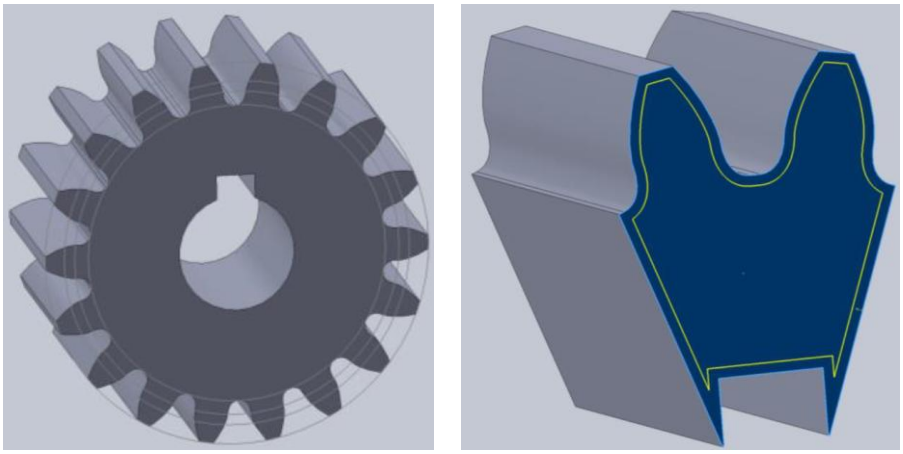

Figure. 2. Studied gear geometry and shape (a) isometric view (b) critical section of the gear

The aim of selecting the critical section of the gear for finite element simulation was to reduce the topology optimization process time. According to the worst-case scenario, if the optimized geometry has the desirable performance for the critical section, the proper performance of the entire gear can be guaranteed because other sections have lower stress concentration and stress distribution values. The topology optimization objective considered to reduce the gear mass by about 70%. After the topology optimization simulation, the obtained results were imported into the Solidworks software. A mesh sensitivity study was conducted to assess the accuracy and convergence of the finite element model by considering various mesh sizes. Different mesh sizes were applied to evaluate the impact of the global mesh size on the obtained results, such as stress distribution and values, to determine the optimal mesh for reliable and efficient analysis. The goal was to identify the mesh size at which the results become independent of further mesh refinement. For this purpose, the global mesh size was reduced from 4 mm (4408 elements) to 0.75 mm (149000 elements) to investigate the stress distribution and values for the TOSG finite element model static carry loading, which will be discussed in section 3.1. Although the stress distribution was the same for all the finite element models with different global mesh sizes, the Von Mises stress values changed remarkably considering various mesh sizes. Figure 3 indicates the Von Mises stress value versus the number of elements for the finite element model. As the global mesh size was reduced, the Von Mises stress values increased from 10.57 to 20 MPa and converged to a stable value. Finite element model convergence was achieved when the global mesh size was 1 mm.

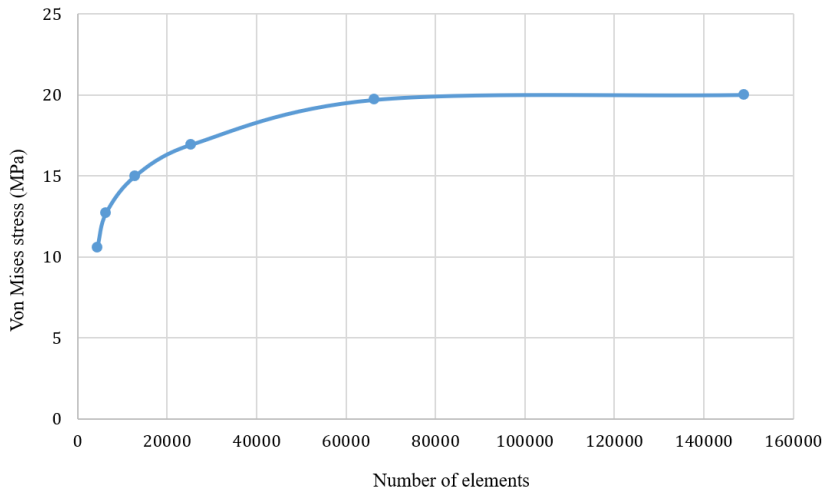

Figure. 3. Mesh sensitivity analysis diagram for the TOSG finite element model static carry loading

The model utilized the C3D8R element, an 8-node linear brick element with reduced integration and hourglass control. This element is commonly used for 3D stress analysis. The C3D8R element offers several advantages, including reduced computational cost due to its reduced integration feature. Additionally, the hourglass control ensured the stability of the model. The element shape was Hex, and the employed meshing technique was Sweep. Using the Sweep technique allowed for an efficient and structured mesh generation, which is crucial in complex geometries such as the TOSG in the presented study.

2.2 Redesign of The Gear's Geometry

In this section, the initially topology-optimized geometry (ITOG) for the critical section was redesined to improve the geometric integrity, reduce the voids in the gear's body, and reduce the manufacturing costs and time. The complexity of the ITOG is shown in Figure 4. According to Figure 4, the cross section of the ITOG consists of various plates with different orientations. Therefore, it is essential to use a simpler geometry for the gear to solve the mentioned problems.

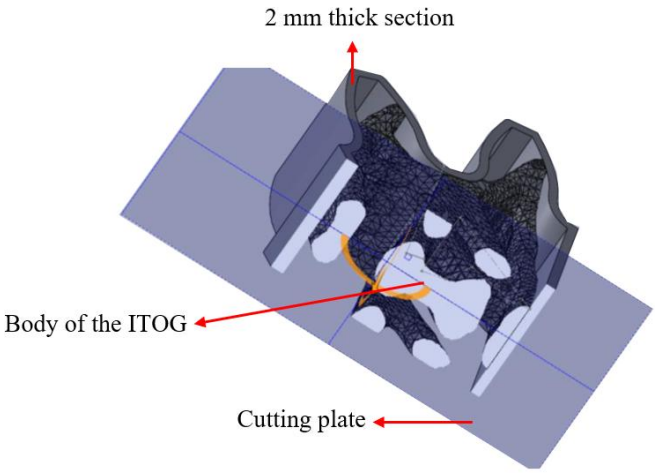

Figure. 4. Presentation of the 2 mm thickness section and complexity of the ITOG model

Besides these, finite element simulation of the ITOG was encountered with various errors in the Abaqus software. Meshing some sections of the ITOG model was found impossible. Furthermore, the gears may be subjected to reversible loading conditions, and the applied force direction may reverse repeatedly. To address these concerns, a geometrically symmetric design for the gear can be beneficial. This issue was considered in the design of the 3D-printed gear in this research.

2.3 Dynamic Performance Consideration

Gear vibrations are mainly caused by external sources such as rotational speed changes and torque fluctuations or internal sources like periodic changes in meshing stiffness and transmission error. Transmission error is considered one of the main characteristics of the dynamic performance of gears, directly showing the gear vibration and noise [17]. As a result, this parameter was explored in many studies related to the dynamic behavior of gears.

Transmission error is the deviation between the actual position of the gear and the expected position based on the defined input rotation of the gear [18]. Meshing stiffness variations are the main reason for transmission error creation in the gears. Therefore, it is crucial to calculate the meshing stiffness in gears to investigate their dynamic performance. However, calculating the meshing stiffness is challenging due to the complicated mechanism of the gear tooth engagement [19]. The meshing stiffness changes with the rotation of gears and the variation in the contact line position between two gears. Gear tooth deformation caused by shear, bending, axial, and contact forces which can change the contact line position in the gears. As a result, the number of engaged tooth pairs during a meshing cycle between two gears varies, leading to sudden changes in the meshing stiffness value. An analytical approach was used to calculate the meshing stiffness in this research. First, the meshing stiffness was estimated for one tooth according to the following equation:

$$\frac{1}{K_{st}} = \frac{1}{K_b} + \frac{1}{K_s} + \frac{1}{K_a} + \frac{1}{K_h} + \frac{1}{K_{rim}} \tag{1}$$

Where K_b, K_s, K_a, K_h, and K_{rim} shows the bending, shear, axial, contact, and rim stiffness. Once the meshing stiffness of each tooth gear is determined, the meshing stiffness at the point where a pair of teeth engage can be obtained using Equation (2):

$$\frac{1}{K_m} = \frac{1}{K_{st1}} + \frac{1}{K_{st2}} \tag{2}$$

Where K_{st1} is the tooth meshing stiffness for the first gear and K_{st2} is the tooth meshing stiffness for the second gear. The meshing stiffness at the point where two pairs of theeth engage is determined by:

$$K_m = \sum_{i=1}^{n} K_{mi} \tag{3}$$

Where the K_{mi} indicates the meshing stiffness of the first and second pair of teeth. İn the analytical approach for meshing stiffness estimation, first, the displacements were calculated. Then, the meshing stiffness was estimated according to the bending, shear, axial, contact, and rim stiffness. İn the next step, the meshing stiffness was determined for one pair of teeth according to Equation (2). Finally, the meshing stiffness for two pairs of teeth was assessed considering Equation (3). Chen et al. [20] calculated the meshing stiffness. The bending, shear, and axial stiffness were determined using Equation (4) to (6), respectively:

$$\frac{1}{K_b} = \int_0^d \frac{(x\cos\alpha_1 - h\sin\alpha_1)^2}{EI_x}\,dx \tag{4}$$

$$\frac{1}{K_s} = \int_0^d \frac{1.2\cos\alpha_1}{GA_x}\,dx \tag{5}$$

$$\frac{1}{K_a} = \int_0^d \frac{(\sin\alpha_1)^2}{EA_x}\,dx \tag{6}$$

Where A_x, I_x, and G are the cross-sectional area, moment of inertia, and shear modulus of the gear tooth, respectively. These parameters were calculated using Equation (7) to Equation (9):

$$I_x = \begin{cases} \frac{1}{12}(h_x + h_x)^3 W & h_x \le h_q \\ \frac{1}{12}(h_x + h_q)^3 W & h_x > h_q \end{cases} \quad (7)$$

$$A_x = \begin{cases} (h_x + h_x)\, W & h_x \le h_q \\ (h_x + h_q)\, W & h_x > h_q \end{cases} \quad (8)$$

$$G = \frac{E}{2(1+\nu)} \quad (9)$$

In this research, it was assumed that the contact stiffness is constant and calculated according to the following equation:

$$K_h = \frac{4(1-\nu^2)}{\pi E W} \quad (10)$$

Furthermore, the rim stiffness was not considered since it has no effect on the contact line of the gears and does not change the meshing stiffness in this study. The other variables mentioned in Equation (4) to Equation (9) were related to the geometry and loading condition of the gears shown in Figure 5. The essential parameters for calculating the meshing stiffness are provided in Table 2.

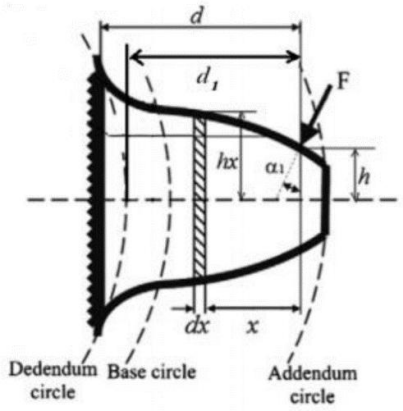

Figure. 5. Schematic representation of the gear tooth as a non-uniform cantilever beam

Table 2 Required parameters for calculating the meshing stiffness of the studied gear

Parameter name	Value
Shear modulus (G)	79 GPa
Young modulus (E)	210 GPa
Force angle (α_1)	20°

Gear width (W)	30 mm
Effective length of the gear (d)	18 mm
Vertical height from the symmetry line to the point of applied load (h)	8.5 mm

Meshing stiffness estimation started with calculating the h_x for the gears. The coordinates of the tooth curve points were measured to obtain the h_x function. Then, different regression models were applied to predict the h_x function. The function with the highest coefficient of determination has the highest accuracy in estimating the target function (h_x) [21]. In the next step, h_x, h_x, and stiffness coefficients were determined sequentially. Finally, the meshing stiffness of paired teeth was explored according to the Equation (2) and (3).

3 Results and Discussion

In this section, we examined the TOSG model by analyzing static carry loading and dynamic performance considerations. The results of the static carry loading are presented in Section 3.1. Section 3.2 discusses the outcomes related to meshing stiffness and dynamic performance in the gear by investigating the NOSG, TOSG, and BFOSG model.

3.1 Static Carry Loading of Topology Optimized Gear

In some power transmission systems, accessing the gears, bearings, shafts, and other components of the power transmission system could be challenging after the installation. Therefore, it is essential to reduce the weight of the gears to minimize the load on various parts of the power transmission system, provided that the carry loading capacity is ensured. We performed the topology optimization procedure to reduce the weight of the gear to one-third of its initial mass. The gear studied in this research was part of a power transmission system with a 50 KW capacity and 99% power transmission efficiency. The input speed of 15 rpm was transmitted to the investigated pinion through another gear. The studied pinion increased the speed by a ratio of 70, resulting in an output speed of 1050 rpm. The transmitted load in this situation is 5000 N, applied to the contact point of the gear in the finite element topology optimization procedure. While the applied load may influence the result of the topology optimization process, the optimization was carried out for the discussed case, and studying the effect of loading values on the topology optimization results was not in the scope of this research. The part of the gear that connects to the shaft was completely fixed without any degrees of freedom except axial rotation. The optimization process objective was defined as minimizing the strain energy. The topology optimization algorithm in the Abaqus software reduced the gear weight from the regions with low-stress values. It continued this process until the defined constraint in the problem was violated. As discussed earlier, the 2 mm thickness section was not considered in the optimization process to maintain the initial shape of the teeth. Figure 6 shows the ITOG for the critical section of the gear.

Figure. 6. The geometry of the gear's critical section in the ITOG model

As discussed in section 2.2, the ITOG model was very complex, and it is critical to redesign the geometry for the critical section of the gear. Therefore, the studied gear was redesigned to provide a simpler geometry for gear by measuring the different dimensions of the ITOG. Figure 7 indicates the final topology-optimized geometry for the gear which considerd as the TOSG model.

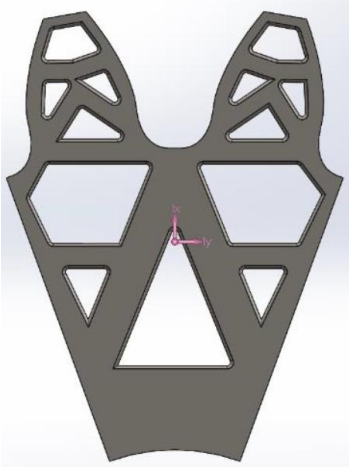

Figure. 7. The geometry of the gear's critical section after redesign stage, considered as TOSG model

After exploring the TOSG model, the TOSG model static carry loading capacity was compared to the NOSG model. A 50 N.m torque was applied to the center point of the gears. The NOSG maximum stress was 7.8 MPa and happened at the point of tooth engagement. The NOSG model weight was 5220 gr. İn the next stage, the 50 N.m torque was applied to the center point of the TOSG model. The stress contours for the engagement tooth can be seen in Figure 8. The maximum Von Mises stress in this case was about 19.7 MPa. The TOSG model weight was reduced to 3445 gr in this case. Although the maximum stress was increased by about 12 MPa which is not significant, the weight of the gear declined to 66% of its initial value. This marked weight reduction can have a significant impact on reducing energy consumption in the transmission systems. Furthermore, the reduction in the gear's weight results in saving a considerable amount of raw material in gear manufacturing. Another important point about the TOSG model is its effective stress redistribution. According to Figure 8, the location of the maximum stress was seen at the main body of the gear which is less critical than the location of the tooth engagement. Thus, topology optimization has not

only reduced the gear's weight significantly but also enhanced the reliable performance of the gear by distributing the stress effectively to the regions with a lower risk of failure.

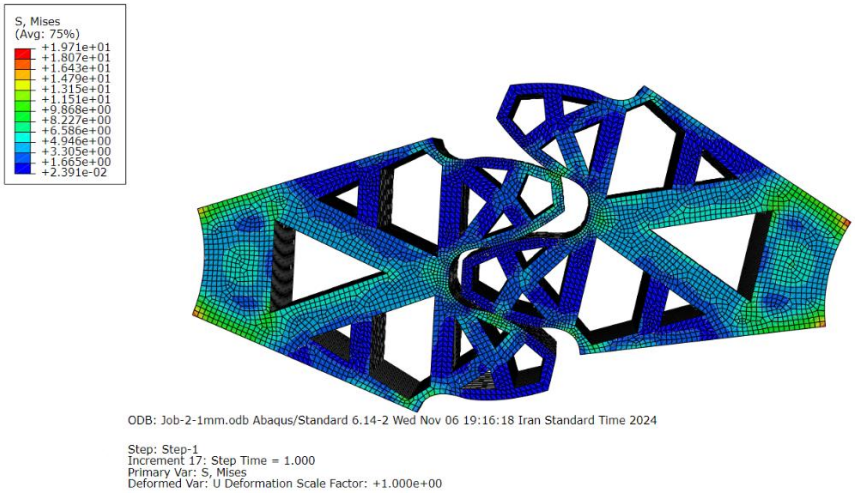

Figure. 8. Finite element analysis of stress distribution for the TOSG model

3.2 Dynamic Performance Consideration of Gear

In this section, the dynamic performance of gears was explored using the meshing stiffness. First, the NOSG model meshing stiffness was extracted. NOSG is a solid spur gear, shown in Figure 2.a. The meshing stiffness estimation started with calculating the h_x function for the gear. We calculated the coordinates of the tooth curve points to obtain the x function. Then, the best regression function estimated the h_x function. The obtained function for the h_x considering NOSG model is:

$$h_x = -1.271 \times 10^7 \times x^5 + 9.69 \times 10^5 \times x^4 - 27940x^3 + 359.95x^2 - 2.1197x + 0.013204 \quad (11)$$

where x and h_x are in meters. Figure 9 indicates the function of actual data points (data1) and fitted function (5th data) for the NOSG model h_x function. According to Figure 9, the fitted function captured the behavior of actual data points accurately and can present the relation between x and h_x very well. After identifying the h_x function, the stiffness values were calculated considering Equations (4) to (6). Table 3 presents the stiffness values and weight of one tooth for this model. In the next step, two modified models were selected and compared to the NOSG model.

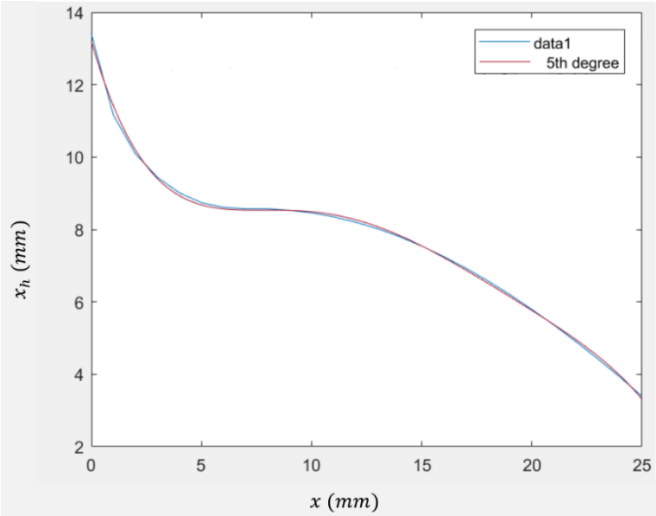

Figure. 9. h_x function form in the NOSG model obtained by regression

The second model studied for the dynamic performance consideration of the gear is TOSG. İn the previous section, the static carry loading of this model was explored. Figure 10.a shows the geometry of one tooth in the TOSG model. Like the previous case, the h_x function must be determined first to calculate the meshing stiffness. However, the challenge in this case is that calculating I_x and A_x is not straightforward using the h_x function because the tooth of the TOSG model contains many hollow regions.

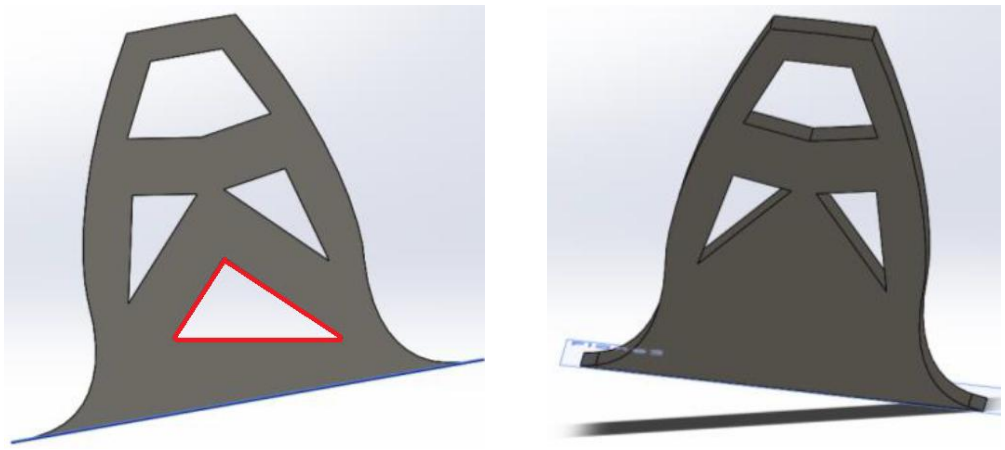

(a) (b)

Figure. 10. Gear teeth geometry in the (a) TOSG model and (b) BFOSG model

Calculating the I_x and A_x was performed directly from the model in this case. For this purpose, cuts were made in the teeth at 1 mm intervals. Then, I_x and A_x were calculated in each cut section for the teeth. Finally, like the NOSG model, appropriate regression models were used to obtain the I_x and A_x functions for the TOSG model. The I_x and A_x functions for the TOSG model are:

$$A_x = 35565x^4 - 1787x^3 - 27940x^3 + 29.609x^2 - 0.1943x + 0.0008 \quad (12)$$

$$I_x = 1.0005x^4 - 0.0539x^3 + 0.001x^2 - 8 \times 10^{-6} \times x + 3 \times 10^{-8} \quad (13)$$

The variables in the above equations are in meters. In the next step, stiffness values were calculated for the TOSG model. The stiffness values and weight of one tooth for this model are presented in Table 3. According to the obtained results, the weight of the tooth is about 76% of the NOSG model and indicates a significant weight reduction. However, the meshing stiffness of the TOSG is 42% of the NOSG. The marked decline in the meshing stiffness value can affect the dynamic performance of the gear and lead to vibration and noise creation. Therefore, the BFOSG model was investigated to solve the low meshing stiffness value for the topology-optimized gears. The geometry of the tooth for the BFOSG model is shown in Figure 10.b. The main difference between the BFOSG and the TOSG models is that in the BFOSG model, the lower part of the tooth, which is a triangle and highlighted in red in Figure 10.a, is filled. Aside from this, all other geometrical and dimensional parameters are the same between the two models. Like the previous case, I_x and A_x were determined using the best-fitted regression model. Then, stiffnesses values were obtained for the model. Equations (14) and (15) represent the I_x and A_x function for the BFOSG model:

$$A_x = 15679x^4 - 713.55x^3 + 10.563x^2 - 0.0782x + 0.0007 \quad (14)$$

$$I_x = -64.304x^5 + 4.71x^4 - 0.1285x^3 + 0.0016x^2 - 9 \times 10^{-6} \times x + 3 \times 10^{-8} \quad (15)$$

According to the obtained results, the weight of the tooth is about 83% of the NOSG model and indicates a relatively significant weight reduction. Furthermore, the meshing stiffness of the BFOSG is 88% of the NOSG model. Although the tooth weight in the BFOSG model is slightly higher than that of the TOSG model, the meshing stiffness is approximately 46% greater. This improvement significantly enhances the dynamic performance of the BFOSG model compared to the TOSG model. Thus, it can be concluded that the BFOSG model is the optimal design for the topology optimization of the studied gear, taking into account dynamic performance. Table 3 presents the stiffness and tooth weight values for this model.

Table 3 Stiffness values and tooth weight for three studied models

Model name	K_b	K_s	K_a	K_h	K_{st}	Tooth weight (gr)
NOSG	2.28×10^6	2.13×10^6	5.14×10^7	5.44×10^6	9×10^5	84.79
TOSG	5.63×10^5	1.52×10^6	3.66×10^7	5.44×10^6	3.78×10^5	64.63
BFOSG	2.35×10^6	1.61×10^6	3.87×10^7	5.44×10^6	7.95×10^5	70.8

4. Conclusion

This study presents a comprehensive analysis of topology optimization in spur gears designed for additive manufacturing, specifically focusing on the static and dynamic performance. Through systematic topology optimization of the gear's critical section, a significant reduction in gear weight was achieved, reducing it by approximately 34% without substantial loss of structural integrity. This weight reduction has substantial implications for enhancing energy efficiency and reducing raw material usage, which aligns well with manufacturing goals.

The study evaluated three models: the non-optimized spur gear (NOSG), the topology-optimized spur gear (TOSG), and the bottom-filled optimized spur gear (BFOSG). Among

these, the TOSG model offered the greatest weight reduction compared to the NOSG model but also revealed a notable decrease in meshing stiffness, raising concerns about dynamic performance. By introducing the BFOSG model, which retained a filled base, the stiffness was increased by about 46% compared to the TOSG model. This improvement demonstrates the BFOSG's ability to maintain dynamic stability with a minimal weight increase compared to the TOSG model, making it a well-suited design for applications where both weight efficiency and dynamic performance are critical.

The findings present the potential of combining topology optimization with additive manufacturing to innovate gear designs that meet both lightweight and high-performance requirements. The BFOSG model, in particular, shows promise as an optimal design for achieving reduced weight without sacrificing the necessary stiffness for dynamic reliability. Future research could expand on these results by exploring various material compositions and further refining the meshing stiffness calculations to optimize performance across a wider range of operational conditions. This study sets a foundation for utilizing advanced manufacturing and optimization techniques in gear design, providing a route toward efficient, sustainable, and high-performance transmission systems.

References

[1] A. García-Domínguez, J. Claver, A. M. Camacho, and M. A. Sebastián, "Analysis of general and specific standardization developments in additive manufacturing from a materials and technological approach," *IEEE Access*, vol. 8, pp. 125056-125075, 2020, doi: https://doi.org/10.1109/ACCESS.2020.3005021.

[2] A. A. Raheem *et al.*, "A review on development of bio-inspired implants using 3D printing," *Biomimetics*, vol. 6, no. 4, p. 65, 2021, doi: https://doi.org/10.3390/biomimetics6040065.

[3] I. Gibson, D. Rosen, B. Stucker, I. Gibson, D. Rosen, and B. Stucker, "Direct digital manufacturing," *Additive manufacturing technologies: 3D printing, rapid prototyping, and direct digital manufacturing*, pp. 375-397, 2015, doi: https://doi.org/10.1007/978-1-4939-2113-3_16.

[4] J. Łuszczek, "Review of methods of designing and additive manufacturing of gears," *Biuletyn Wojskowej Akademii Technicznej*, vol. 70, no. 2, 2021.

[5] M. Kluge, G. Kotthoff, C. Cavallini, G. Driveline, S. Höges, and G. Metallurgy, "Design and production of innovative transmission components with additive manufacturing," in *Proceedings of the 16th International CTI symposium automotive transmissions, HEV and EV drives, Berlin, Germany*, 2017, pp. 5-7.

[6] L. Pujari, S. Manoj, O. K. Gaddikeri, P. Shetty, and M. B. Khot, "Recent advancements in 3D printing for gear design and analysis: a comprehensive review," *Multiscale and Multidisciplinary Modeling, Experiments and Design*, pp. 1-25, 2024, doi: https://doi.org/10.1007/s41939-024-00529-w.

[7] K. Gupta, "Recent developments in additive manufacturing of gears: A review," *Advances in Manufacturing Technology XXXII*, pp. 131-136, 2018, doi: https://10.3233/978-1-61499-902-7-131.

[8] A. J. Muminovic, N. Pervan, M. Delic, E. Muratovic, E. Mesic, and S. Braut, "Failure analysis of nylon gears made by additive manufacturing," *Engineering failure analysis*, vol. 137, p. 106272, 2022, doi: https://doi.org/10.1016/j.engfailanal.2022.106272.

[9] J. Yang, Y. Zhang, R. Li, and C.-H. Lee, "Characterization of damping in 3D metal printed gear body using parameter optimization," *Journal of Vibration and Control*, vol. 30, no. 13-14, pp. 3220-3232, 2024, doi: https://doi.org/10.1177/10775463231192725.

[10] C. Moldovan and C. Sticlaru, "Performance Analysis of Polymer Additive Manufactured Gear Bearings," *Applied Sciences*, vol. 13, no. 22, p. 12383, 2023, doi: https://doi.org/10.3390/app132212383.

[11] D. Brackett, I. Ashcroft, and R. Hague, "A dithering based method to generate variable volume lattice cells for additive manufacturing," 2011.

[12] L. Cheng, P. Zhang, E. Biyikli, J. Bai, J. Robbins, and A. To, "Efficient design optimization of variable-density cellular structures for additive manufacturing: theory and experimental validation," *Rapid Prototyping Journal*, vol. 23, no. 4, pp. 660-677, 2017, doi: https://doi.org/10.1108/RPJ-04-2016-0069.

[13] E. Tyflopoulos, M. Lien, and M. Steinert, "Optimization of brake calipers using topology optimization for additive manufacturing," *Applied Sciences*, vol. 11, no. 4, p. 1437, 2021, doi: https://doi.org/10.3390/app11041437.

[14] B. Becergen, M. Cakmak, M. F. Maral, A. Dayanc, and F. Karakoc, "Design approaches on inner bodies of gears with methods topology optimization and lattice structures," *Avrupa Bilim ve Teknoloji Dergisi*, no. 39, pp. 85-90, 2022, doi: https://doi.org/10.31590/ejosat.1144818.

[15] M. Patel, H. Valiulla, V. Khatod, B. Chaudhary, and V. Gondalia, "Topology Optimization of Automotive Gear using Fea," *International Journal of Recent Technology and Engineering*, vol. 8, no. 4, pp. 1079-1084, 2019.

[16] R. Ramadani, A. Belsak, M. Kegl, J. Predan, and S. Pehan, "Topology optimization based design of lightweight and low vibration gear bodies," *International Journal of Simulation Modelling*, vol. 17, no. 1, pp. 92-104, 2018, doi: https://doi.org/10.2507/IJSIMM17(1)419.

[17] M. Pimsarn and K. Kazerounian, "Efficient evaluation of spur gear tooth mesh load using pseudo-interference stiffness estimation method," *Mechanism and machine theory*, vol. 37, no. 8, pp. 769-786, 2002, doi: https://doi.org/10.1016/S0094-114X(02)00022-8.

[18] A. F. Del Rincon, F. Viadero, M. Iglesias, P. García, A. De-Juan, and R. Sancibrian, "A model for the study of meshing stiffness in spur gear transmissions," *Mechanism and Machine Theory*, vol. 61, pp. 30-58, 2013, doi: https://doi.org/10.1016/j.mechmachtheory.2012.10.008.

[19] R. Parker, S. Vijayakar, and T. Imajo, "Non-linear dynamic response of a spur gear pair: modelling and experimental comparisons," *Journal of Sound and vibration*, vol. 237, no. 3, pp. 435-455, 2000, doi: https://doi.org/10.1006/jsvi.2000.3067.

[20] Z. Chen and Y. Shao, "Dynamic simulation of spur gear with tooth root crack propagating along tooth width and crack depth," *Engineering failure analysis*, vol. 18, no. 8, pp. 2149-2164, 2011, doi: https://doi.org/10.1016/j.engfailanal.2011.07.006.

[21] H. Soroush and A. Nourani, "Application of data mining techniques for assessment of fracture load and energy in double cantilever beam solder joints," *Journal of Design Against Fatigue*, vol. 1, no. 3, 2023, doi: https://doi.org/10.62676/9v4azj82.

THE UTILIZATION OF 3DP IN MISWAK HOLDER FABRICATION

Sharuddin BinMohd Dahuri[1], Nor Hakimah Binti Ahmad Subri[2], Aliff Bin AB Tahir[3], Abu Harfiz Bin Hassan[4].

[1]Politeknik Kuching Sarawak, Kuching Sarawak, Malaysia, sharuddinpks@gmail.com.
[2]Politeknik Kuching Sarawak, Kuching Sarawak, Malaysia, ujiuddin@gmail.com.
[3]Politeknik Kuching Sarawak, Kuching Sarawak, Malaysia, alifftahir24@gmail.com
[4]Politeknik Kuching Sarawak, Kuching Sarawak, Malaysia, abuharfiz@poliku.edu.my

Abstract

Miswak is a traditional tool for cleaning teeth from the trunk of the Salvadora persica tree. It is effective in maintaining overall oral hygiene, as it contains cleaning materials and helps remove dental plaque. Awareness of the benefits of miswak has increased over the past few years, and this shows that there are people who are becoming more and more aware of the benefits of miswak. The force of 5 Newtons was taken for the study because it is related to many human activities that involve motion. When a person walks at a moderate pace, the force exerted on their legs and body can reach a value similar to 5 Newtons or more. Furthermore, previous studies have shown that excessive stress can have negative effects on gums and tooth enamel. The development of the "Siwak holder (Siwak-der)" begins with the design of a digital model using CAD software. Setting FEA test parameters, Software: Autodesk Inventor Professional 2022, material: ABS resin, load center: center and slope 45^0 in the miswak area. For continuous stress (Siwak-der 2 and 3) the material achieves a continuous stress of less than 5.0 Mpa. In addition, indicators (Siwak-der 2 and 3) do not show the maximum effect of stress. Therefore, it is thought that Siwak-der 2 and 3 will be able to meet the required power. For angled force, (Siwak-der 3) achieves a angled stress of less than 5.0 Mpa. It also (Siwak-der 3) does not show maximum stress. Therefore, it has been calculated that Siwak-der 3 will be able to accommodate the required force. Direct stretching and properly controlled angled force will ensure effective cleaning without harming oral health. From a sustainability point of view, miswak, which replaces polymer toothbrushes, brings great benefits to the environment. Studies show that environmental awareness pushes more individuals to choose miswak. For this reason, it is necessary to develop studies to support the use of miswak. Studies have shown that polymers can be used as a base material for the production of miswak supports in 3D printers. The initial cost of producing a product on a small scale can be quite high. But if undertaken on a large scale, it can overcome the following financial problems.

***Keywords*:** Miswak, newton, sustainability.

1. Introduction

The purpose of this study is to provide an overview of the product referred to or referred to as "Siwak-der", which is the siwak holder produced using three-dimensional printing technology. Miswak is traditionally used as a tool for brushing teeth in many cultures, especially among Muslim communities. However, traditional forms of miswak are often less practical, difficult to carry, and inconvenient for long-term use.

The objectives of the study are as follows; i) Produce a model as the basic form of the miswak wooden handle. i) Producing a prototype that functions as a wooden handle for miswak. ii) Determine the allergic pressure and stress of the product produced. Therefore, this study evaluates the potential use of 3D printing in the production of a more comfortable, user-friendly and aesthetic Siwak-der. 3D printing technology allows the creation of products with complex designs tailored to the user's needs, with the introduction of modulation elements for various dimensions and designs that suit the shape of the hand and the needs of the user.

2. Lıterature Revıew

Introducing Toothpicks As A Dental Hygiene Tool

Miswak is a traditional tool used to clean teeth, derived from the trunk of the Salvador Percica tree, known as the toothpick tree. This tool has been used for centuries in the Central Asian region and the Middle East, specifically in Islamic traditions. Miswak is not only a beloved oral hygiene tool for its simplicity, but it is also considered an annual practice in Islam. The Prophet Muhammad (peace and blessings of Allah be upon him) himself reportedly strongly recommends the use of siwak to keep oral and dental hygiene, and Muslims have used it since ancient times.

In some countries, such as Saudi Arabia, Egypt and Central Asian countries, miswak is still widely used as an effective means of dental hygiene, especially among those who prefer natural ways. Miswak is made from the branches of the Salvadora persica tree, which is rich in active ingredients, making it a very useful tool in oral care.

Antibacterial Effects of Miswak

In addition to serving as a mechanical cleaner, miswak is also known for its antibacterial effects. Miswak stems contain active ingredients such as fluoride, salvadorin, and chlorides, which have been proven to have antibacterial properties that can inhibit the growth of harmful bacteria in the mouth (Zulfikar et al., 2014)[1]. Microbological studies have also shown that miswak extract can kill various types of pathogenic bacteria that cause gum disease, dental plaque, and other oral problems such as Streptococcus mutans and Porphyromonas gingivalis (Mohammad et al., 2018)[2].

These antibacterial properties make miswak effective in preventing bad breath (bad breath) and reducing the risk of plaque buildup caused by bacteria in the mouth.

Studies show that miswak has the ability to eliminate dental plaque, provide a powerful antibacterial effect, and support overall gum health. In addition, miswak offers advantages over modern toothpastes in terms of chemical-free natural ingredients and minimal side effects. With oral health practices increasingly emphasizing the use of natural ingredients, miswak continues to be a good choice for dental and oral care.

Previous Studies On General Awareness.

Public awareness of the advantages of miswak over polymer toothbrushes (regular toothbrushes made of plastic with nylon bristles) has increased in recent years, especially among people looking for more natural or organic-based alternatives to oral care. Survey studies conducted in various contexts show that there are segments of society that are increasingly aware of the benefits of miswak, both in terms of oral health and its environmentally friendly effects. In this section, we will discuss how previous survey studies have provided insight into this awareness and how it relates to previous studies that support the findings.

General Awareness Of The Advantages Of Miswak.

Based on survey studies conducted in various cultural and geographical contexts, awareness of miswak as an alternative to toothbrushes is increasing. Although polymer toothbrushes are still more widely used, research has shown that there is a growing interest in misvaka, especially among communities that value the use of natural materials and eco-friendly alternatives. Some of the factors that influence this awareness are:

a. Environmental Impact Awareness

Miswak has a great advantage in terms of environmental friendliness, as it is a natural product that does not involve the production of plastic or synthetic materials. In a survey study by Abdulwahed et al. (2020)[3], there was an increase in awareness among respondents in terms of the negative impact of the use of polymer toothbrushes on the environment, especially plastic pollution. This shows that segments of society that are increasingly concerned about environmental problems are starting to turn to missal as a more environmentally friendly.

b. Effectiveness in Oral Health

A survey study conducted by Al-Maweri et al. (2018) [4] among university students in Yemen showed that almost 70% of respondents knew that miswak had better oral health benefits, especially in reducing dental plaque and gingivitis. Although not all participants routinely use miswak, the majority showed awareness of its effectiveness in maintaining oral hygiene naturally without the need for additional chemicals found in modern toothpaste.

c. Tradition and Culture

This awareness is also influenced by the traditions and cultures in a particular community. In the countries of the Middle East and South Asia, miswak has traditionally been used for centuries, and a survey study by Al-Hashmi et al. (2004) [5] showed that more than 80% of respondents to their study in Arab countries still regularly use miswak as a daily oral hygiene practice or as a religious practice.

Previous survey studies have shown increased public awareness of the advantages of miswak over polymer toothbrushes, especially in terms of its positive effects on oral health and the environment. While polymer toothbrushes remain the best option, miswak is gaining more and more ground among those looking for a more natural and effective alternative. This awareness stems from having a better knowledge of the antibacterial, anti-inflammatory, and environmental protection benefits that miswak has.

3d Printing Technology

A 3D printing machine is a manufacturing technology that creates three-dimensional objects layer by layer based on digital models (CAD). This process is known as additive printing because it creates an object from a material stored in the form of powder, filament, or resin by adding layers of material without shrinking the material as in a traditional machining process. 3D printing technology allows for the production of objects with highly complex and customized geometries, making it a very powerful tool in the manufacturing, prototyping, and medical application.

3D Printing Applications In Industry.

1. User product manufacturing industry.

3D printing allows for the production of more customized and cheaper consumer products. In the fashion and electronics industries, 3D printing is used to produce prototypes faster and cheaper than traditional manufacturing techniques. Nike and Adidas, for example, use 3D printing to print shoe parts tailored to athletes' needs, improving comfort and performance.

1. **Medical Device Industry**

- 3D printing has a wide range of applications in the medical field, including the production of implants, prosthetics and orthodontic devices. Using biocompatible materials, 3D printing allows for the production of medical devices that are completely tailored to the needs of the patient.
- Dental implants, prostheses (prosthetic legs, prosthetic hands) and 3D anatomical models are used to design the surgery more precisely. This minimizes the risk of complications and increases patient comfort.
- Research shows that printed 3D models of anatomy can better assist surgical procedures and provide visual guidance to surgeons (Morrow, 2020)[6].

2. Dental Instruments

- In dentistry, 3D printing is used to produce more customized orthodontic instruments and dentures. These include lighter and more comfortable braces and dentures, which are made to precisely shape patients' gums and teeth.
- Studies have shown that 3D printing in dental instrument manufacturing speeds up the manufacturing process and reduces costs compared to traditional methods (Pantani et al., 2016)[7].

2. Advantages of 3D Printing in Product Manufacturing

1. **Cheaper Cost**
    - 3D printing reduces production costs by eliminating the need to make tools and molds, which are often expensive in mass production. Prototype production is also becoming cheaper and faster, making it the best option for design testing and manufacturing of small products (Gibson et al., 2015)[8].
2. **Faster Process**
    - 3D printing allows for faster product production because it does not require complex processes such as mold manufacturing or long-term modifications. In prototyping, this process speeds up design testing by reducing the time from design to product manufacturing (Gibson et al., 2015)[8].
3. **Better Tailored**
    - One of the main advantages of 3D printing is that it can produce products that are tailored to the user's needs. In medicine, for example, prosthetics and implants can be made based on the patient's personal size and needs, which increases comfort and fit (Morrow, 2020)[6].

Relevance Of Newtonian Force To People And Daily Activities.

Force is a measure of action that causes an object to move or change the direction of its motion. In the human context, we often engage in various activities that require force to start, stop, or change the direction of our movements. A force as simple as 5 Newtons may not be very large on the scale of the physical world, but it still has a significant impact on the human body in various situations;

- The force of 5 Newtons (N) is taken because it is a measure of quantity used in physics to describe force or gravity. In comparison, this force is almost equal to the weight of an object with a mass of about 0.5 kilograms located on the Earth's surface, where the force of gravity is about 9.8 m/s^2.
- The force of 5 Newtons may seem small, but it is related to many human activities that involve movement. Here are some examples that relate this force to human daily activities:
- Walking or Running: When walking or running, the human body reacts to the forces exerted by the earth's surface and gravity. When a person walks at a moderate pace, the force exerted on their legs and body can reach a value similar to 5 Newtons or more. This allows them to move steadily and overcome obstacles such as uneven surfaces.
- Heavy Lifting: The force applied when lifting an object weighing about 0.5 kg will produce a force of about 5 Newtons. For example, when a person lifts a school bag or a moderately heavy shopping bag, he interacts with this force.
- Vehicles and Equipment: In everyday activities, such as riding a bus or car, the force of 5 Newtons can be associated with the force exerted by the hand holding the door handle to maintain balance while the passenger is in the seat or in motion.

In everyday situations, this small acceleration can be seen when we start moving after standing or when accelerating a vehicle. Daily activities that involve interaction with force are important because they affect our physical health. For example, when lifting an object, we use

muscular force to produce a response that moves the object. The force of 5 Newtons may seem like a low ratio, but it is significant enough to affect our physical activity.

Newton's 5 forces play an important role in explaining how we move in the context of human beings and daily activities, interacting with our objects and our environment. While it's not a huge force, it does provide an insight into how the fundamental principles of physics, such as Newton's Laws, apply in our daily lives. Therefore, understanding the forces exerted in daily activities is important to improve our understanding of the forces involved in our actions.

2. Material and Methods

Model Design And Development.

The development process of the miswak holder, known as the "Siwak holder" (Siwak-der)", will begin with the design of a digital model using CAD (Computer Aided Design) software. The following are the basic dimensions of a miswak produced with a 3D printing machine. It should be noted that the dimensions of the siwak-der connection are not critical, as it only provides a platform for the siwak-der to be joined with the hand handle. Connector only serves as a space for the user to hold the tool.

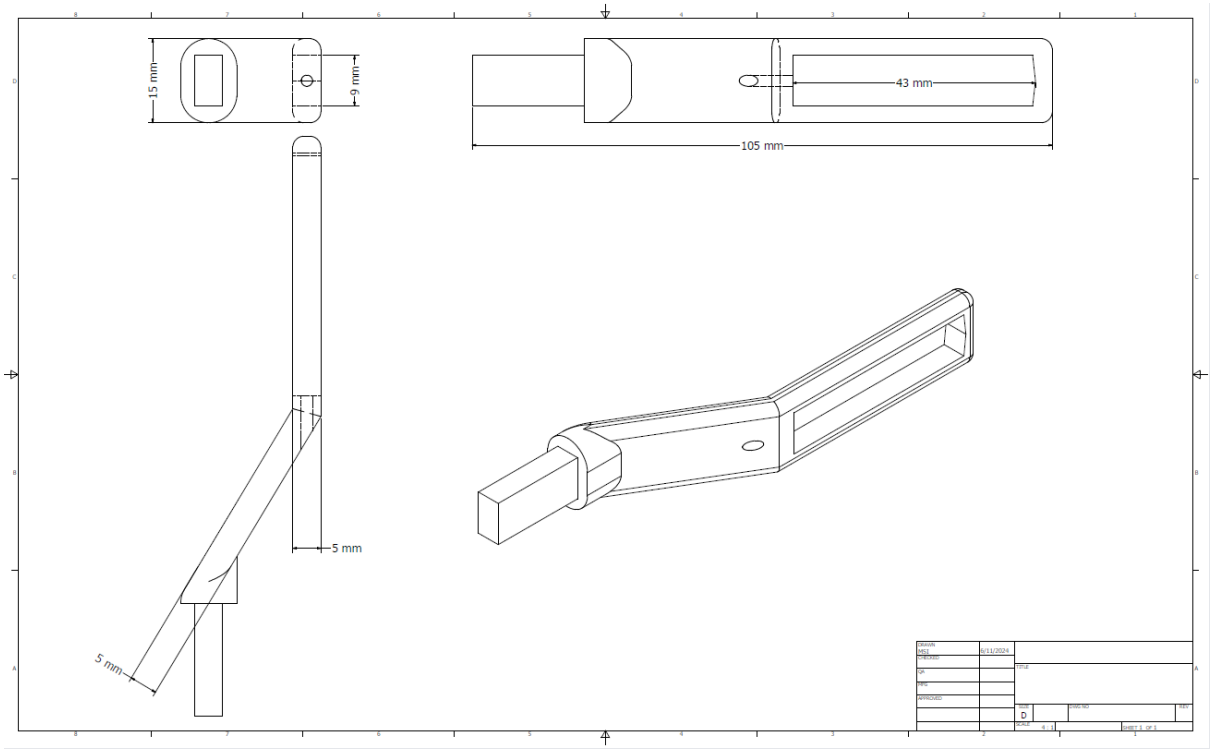

Fig. 1 Dimensi of Siwak-der A

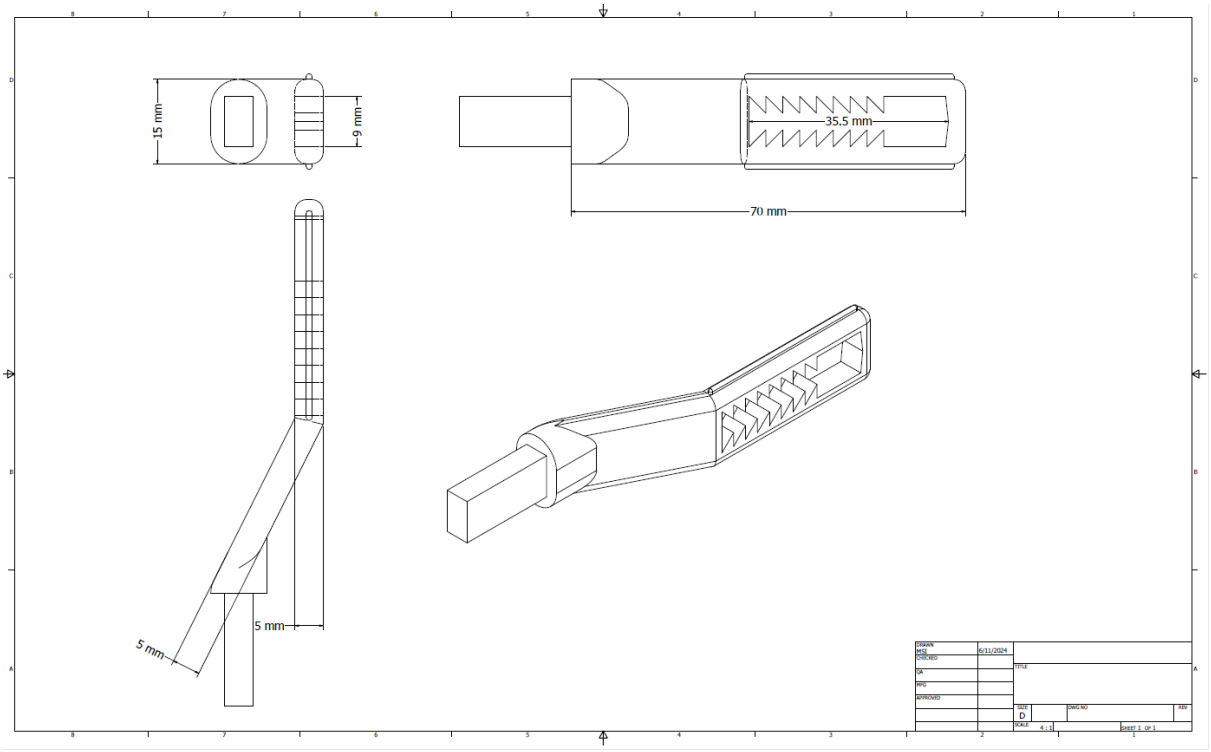

Fig. 2 Dimensi Siwak-der B

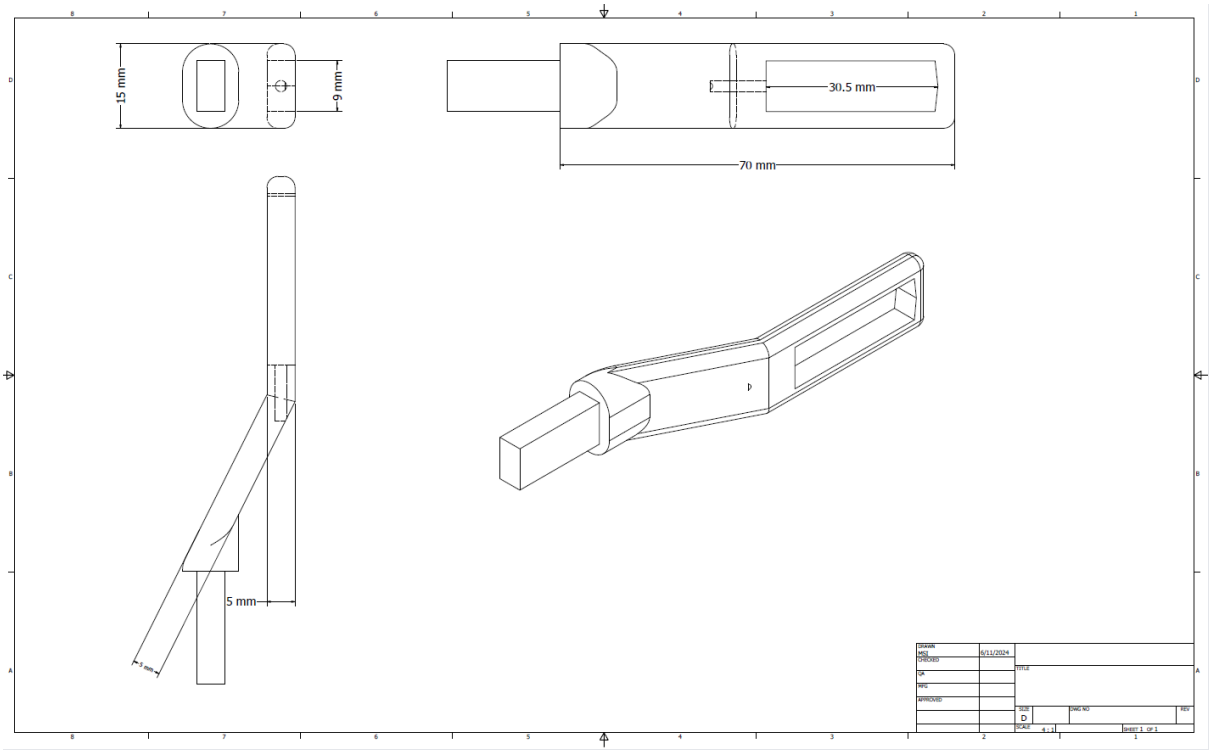

Fig. 3 Dimensi Siwak-der C

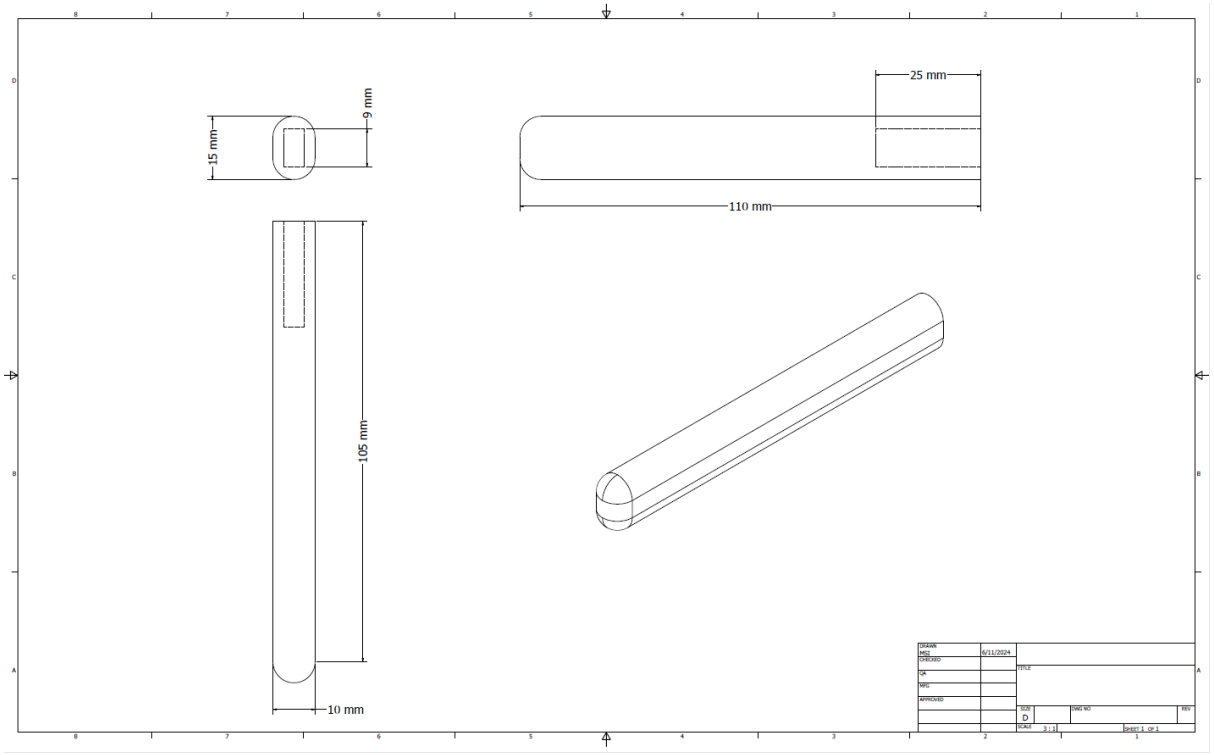

Fig. 4 Dimensi of Siwak-der connector.

Tests And Assessments

The resulting prototype will be tested to evaluate functionality. The test involves using FEA with actual values to get feedback on the design and durability of the Siwak-der.

Initial FEA test parameters include:

Software	: Autodesk Inventor Professional 2022
Material	: ABS Resin 1.75mm, Temperature 200 – 260C, 062777ABS9911
Load Capacity	: 5 N (~0.509 kg).
Load center	: The center of the Miswak installation area.
Rigid position	: Body insertion slot (Connection. Siwak-der).

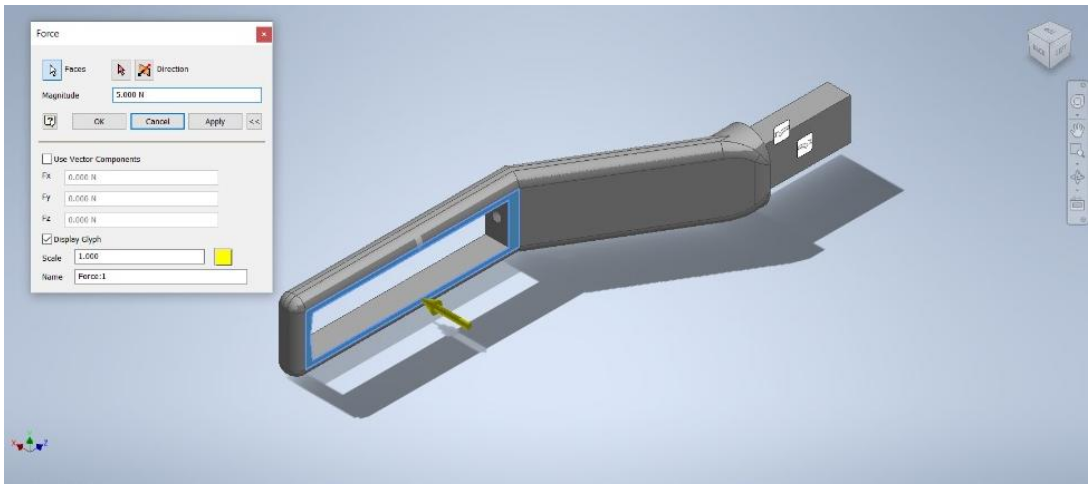

Fig. 5 First FEA parameter setting for Siwak-der A.

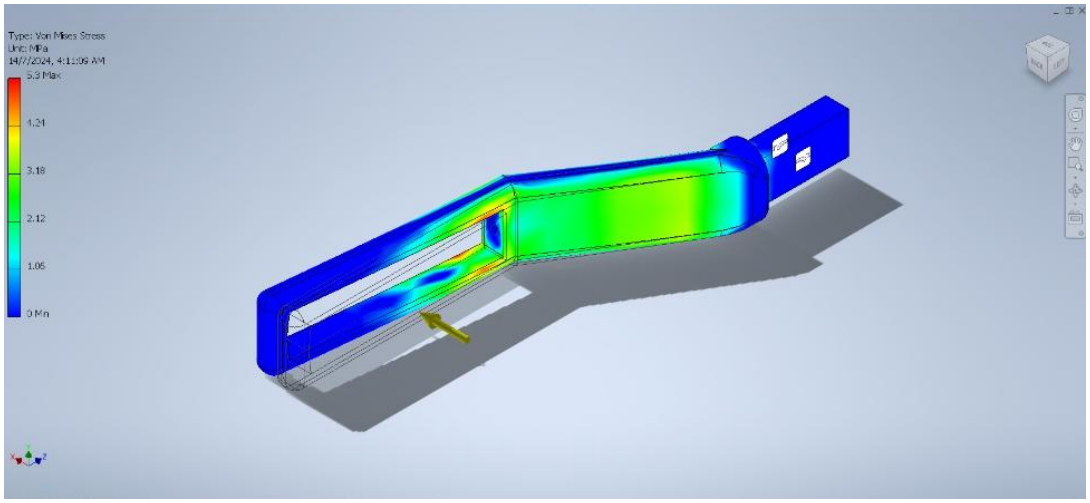

Fig. 6 Siwak-der A, Maxsimum Stress = 5.3 Mpa.

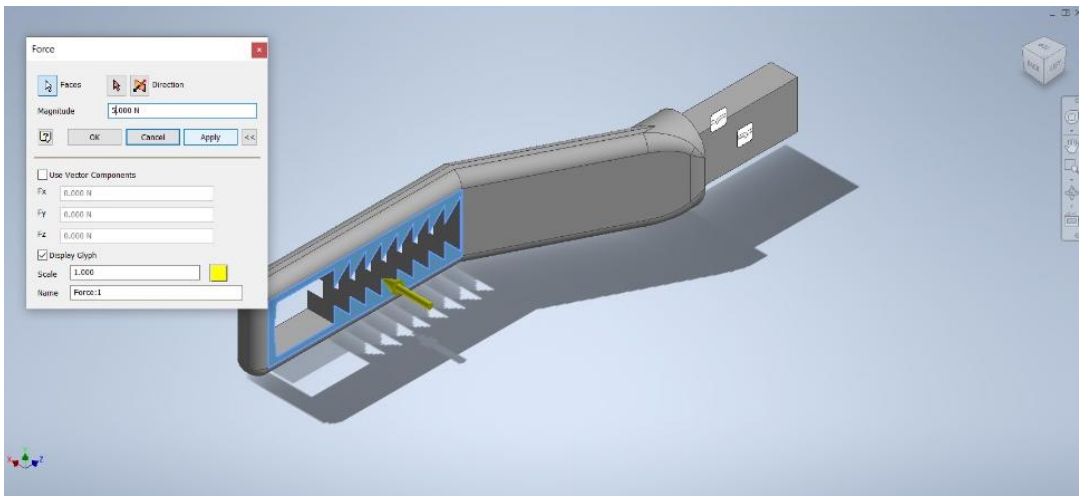

Fig. 7 First FEA parameter setting for Siwak-der B.

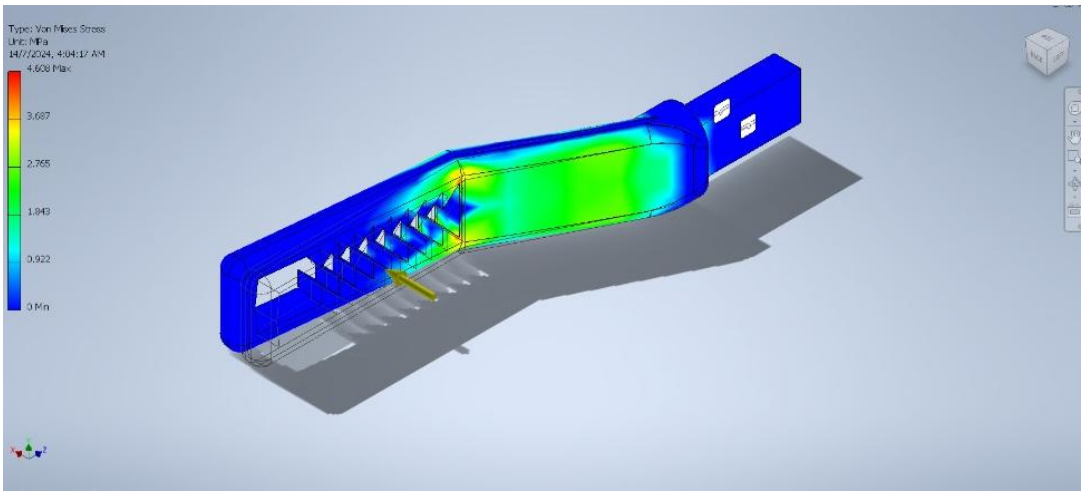

Fig. 8 Siwak-der B, Maxsimum Stress = 4.608 Mpa.

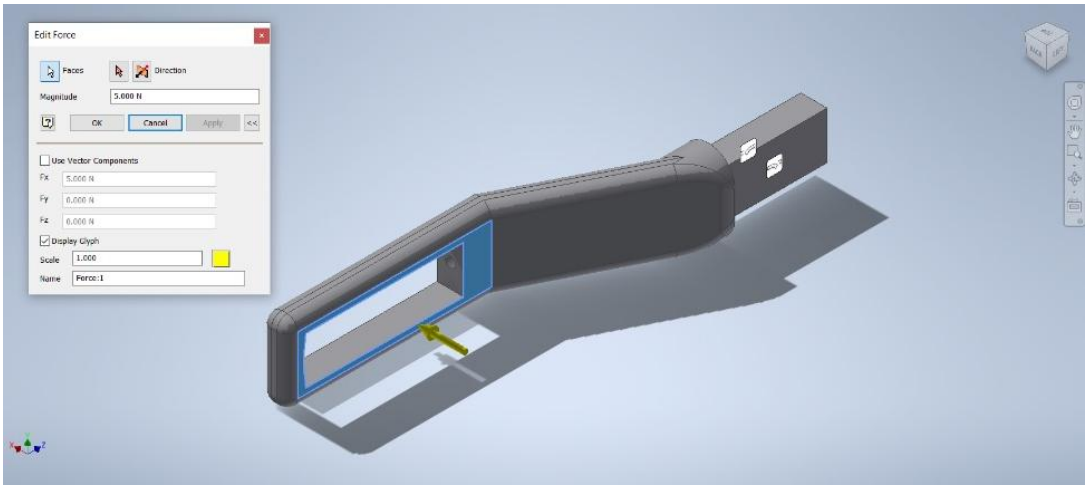

Fig. 9 First FEA parameter setting for Siwak-der C.

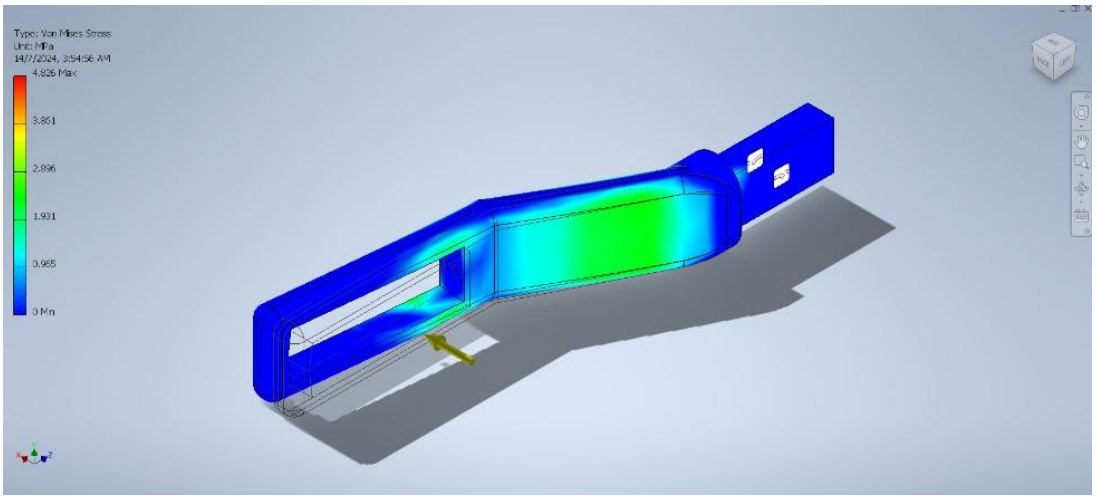

Fig. 10 Siwak-der C, Maxsimum Stress = 4.826 Mpa.

Fig. 11 Siwak-der manual testing.

The second test involves using FEA with actual values to get feedback on the design and effectiveness of Siwak-der. Some of the initial FEA test parameters are as follows:

Software	: Autodesk Inventor Professional 2022
Material	: ABS Resin 1.75mm, Temperature 200 – 260C, 062777ABS9911
Load Capacity	: 5 N (~0.509 kg) @ 45 degree angle.
Load center	: The center of the Miswak installation area.
Rigid position	: The upper right slot of the rod connection.

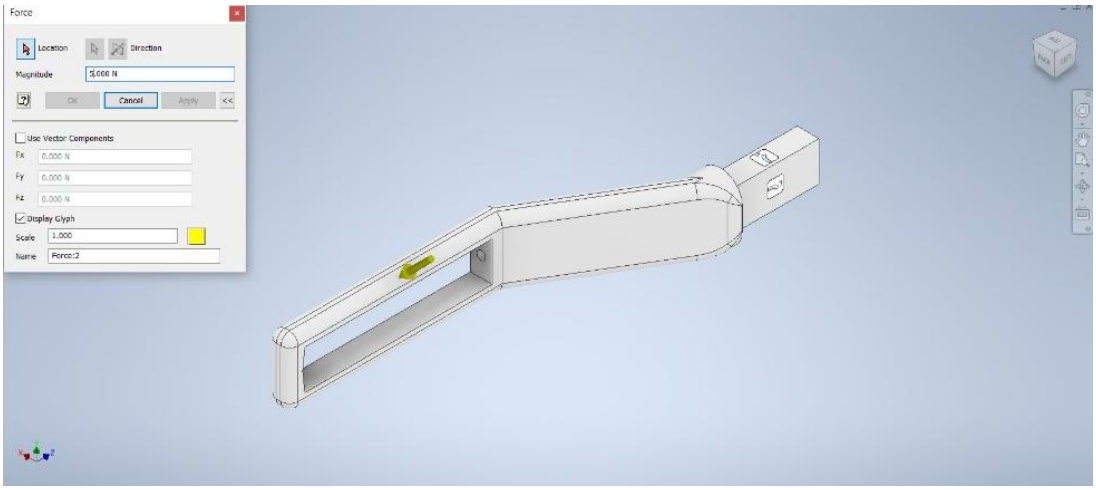

Fig. 12 Second FEA parameter setting for Siwak-der A.

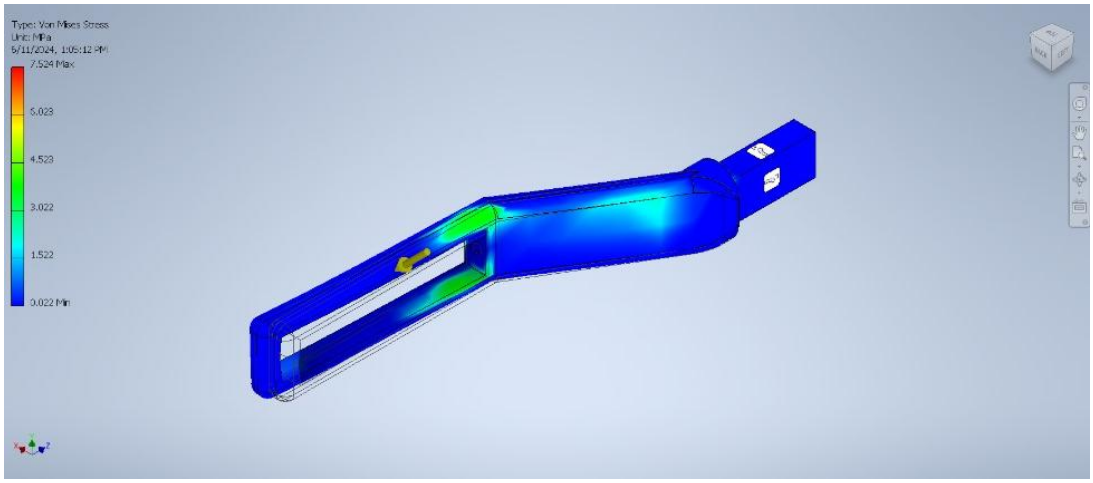

Fig. 13 Siwak-der A, Maxsimum Stress = 7.524 Mpa.

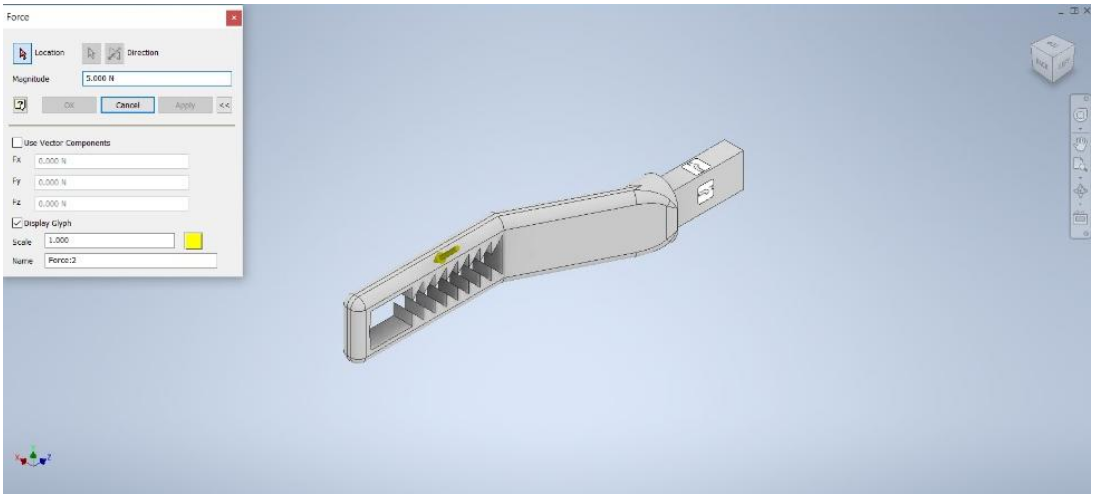

Fig. 14 Second FEA parameter setting for Siwak-der B.

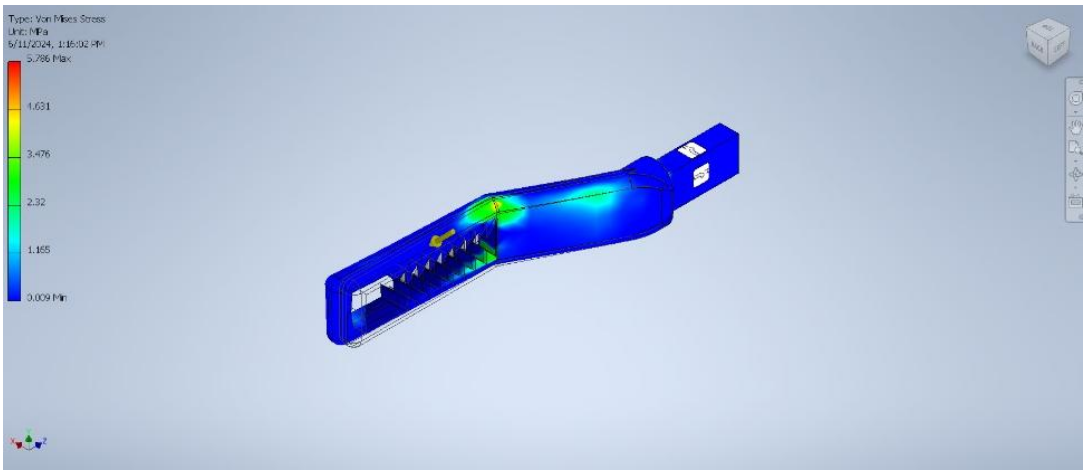

Fig. 15 Siwak-der B, Maxsimum Stress = 5.786 Mpa.

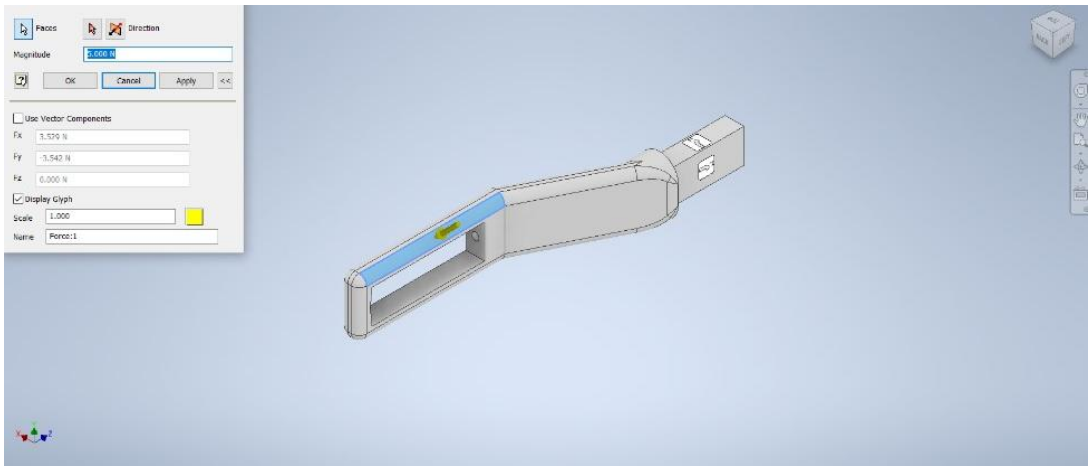

Fig. 16 Second FEA parameter setting for Siwak-der C.

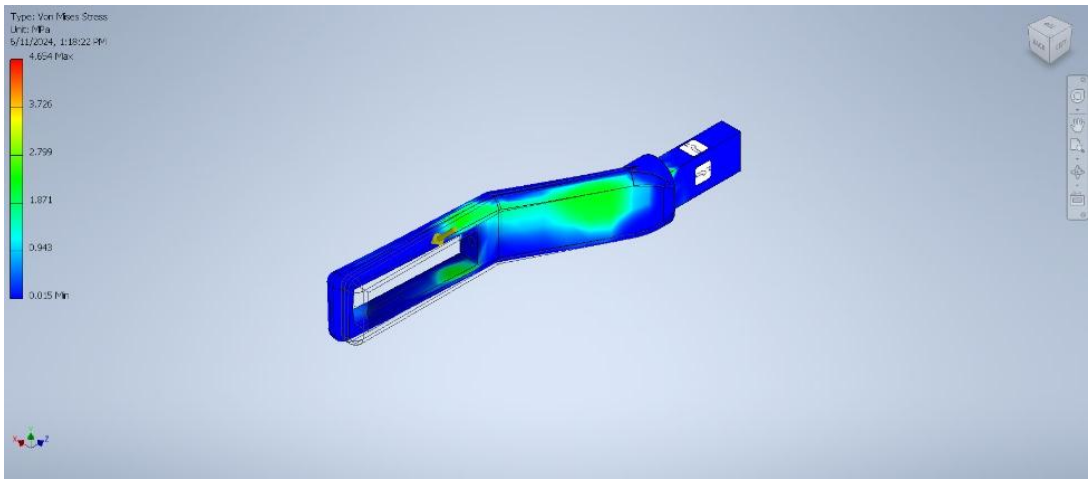

Fig. 17 Siwak-der C, Maxsimum Stress = 4.654 Mpa.

Prototype Printing

After the design of the model is finished, it is printed using a 3D printing machine as follows;

3D printer	: Creality Ender – 3 S1
Raw feed material	: ABS resin 1.75mm, Temperature 200 – 260, 062777ABS9911.
Platform temperature	: 60 mm
Nozzle Temperature	: 200
Fan speed	: %100
Printing Software	: Ultimaker Cura 3.5.0

Fig. 18 Example of some prototype that been printed.

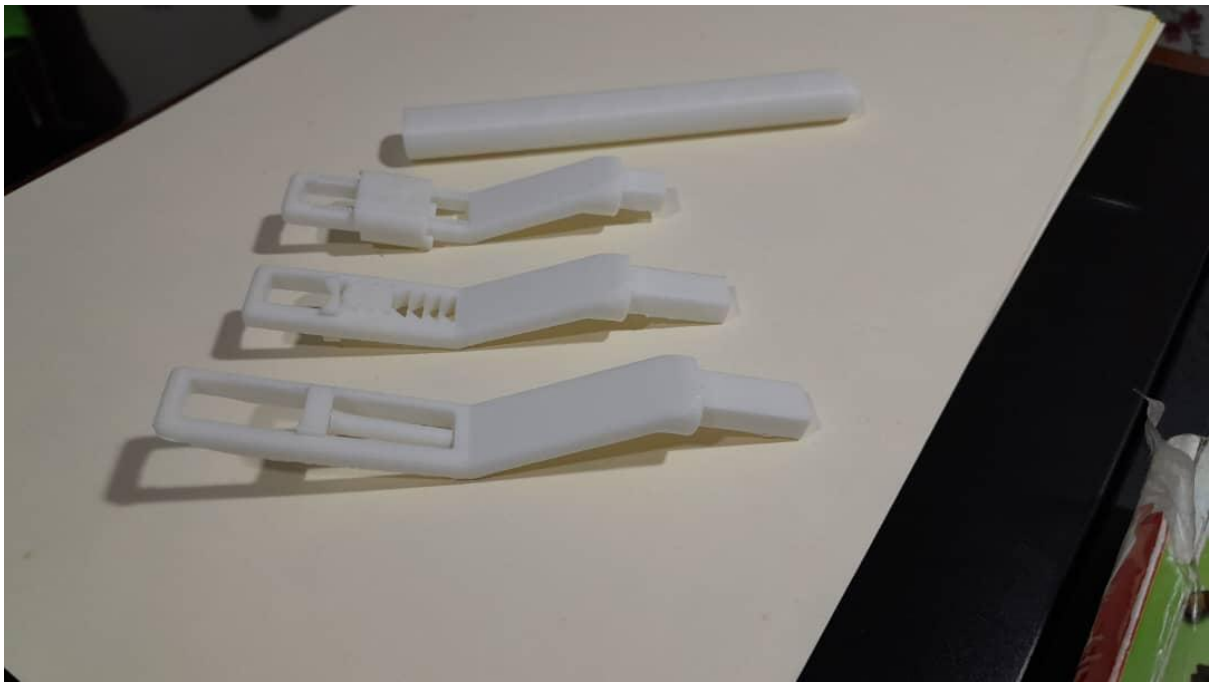

Fig. 19 Comparison of all Siwak-der.

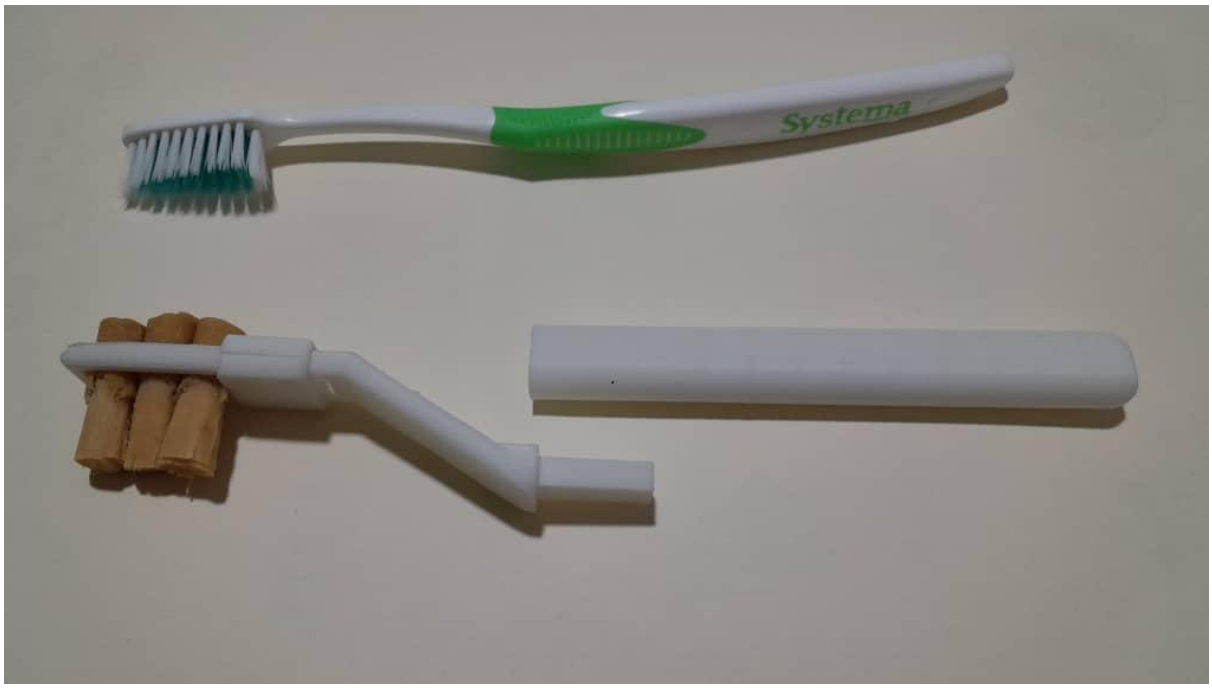

Fig. 20 Comparison of Siwak-der to a normal toothbrush.

4. Discussion

To delve deeper into Siwak-der in relation to the forces involved in the production of toothbrushes, we need to distinguish between direct force and cutting force in the context of toothbrush use. We will briefly explain these two types of tension and give the values of force measurements commonly used for toothbrushes.

1. Direct Stress.

Direct stress refers to the force applied directly to the surface in a perpendicular direction, such as when a person presses the toothbrush against the surface of the teeth and gums. This emphasis serves to clean the surface of the teeth by removing accumulated plaque or dirt.

- Direct force is the force exerted on the teeth during brushing
- Higher direct stress strength can damage tooth enamel if it's too strong or cause gum irritation if pressed too hard.

2. Angled force.

Angled force occurs when the force is applied in a horizontal direction or parallel to the surface. In the context of a toothbrush, this cutting stress occurs when the bristles of the brush touch the surface of the teeth to remove plaque or dirt and slip.

- Angled force strength is also required to more effectively scrape plaque and debris from the tooth surface.
- This angled force plays a greater role in moving dirt on the surface of the teeth than in compressing or compressing the tooth structure itself.

Angled force occurs when the force is applied in a horizontal direction or parallel to the surface. In the context of a toothbrush, this cutting stress occurs when the bristles of the brush touch the surface of the teeth to remove plaque or dirt and slip.

- Angled force strength is also required to more effectively scrape plaque and debris from the tooth surface.
- This angled force plays a greater role in moving dirt on the surface of the teeth than in compressing or compressing the tooth structure itself.

3. Effective Toothbrush Force.

The force applied during the use of the toothbrush is usually within a certain range to ensure effectiveness without damaging the teeth or gums. Based on the study, the recommended force for toothbrush use is as follows:

- The direct force during the use of the toothbrush is recommended to be in the range of 0.5 to 1.5 Newton (N) (Robinson et al., 2005)[9].
- Angled force depends on the type of toothbrush and the technique of use. For example, the force exerted in gentle brushing techniques is lower, about 0.3 to 0.7 N per square centimetre on the tooth surface (Hyatt et al., 2009)[10].

These studies show that excessive pressure can have negative effects on the gums and tooth enamel. Therefore, it is more advisable to use a softer toothbrush with controlled force. To ensure that Siwak-der can work, some data comparisons are presented, as shown in the table below.

Data analysis.

Referring to the above experimental data, the comparison of results can be divided into two types of stress. The first voltage refers to the direct voltage, and the second voltage refers to the oblique voltage.

Table 1 Direct and Angled Force of Siwak-der FEA.

		Direct Force.	Angled Force
Previous Data.	Minimum force.	0.5 N	0.3 N
	Maximum force.	1.5 N	0.7 N
Maximum Stress (FEA)	Safety factor	3	7
	Force setting.	5.0 N	5.0 N
	Siwak-der A	5.300 Mpa	7.524 Mpa
	Siwak-der B	4.608 Mpa	5.786 Mpa
	Siwak-der C	4.826 Mpa	4.654 Mpa

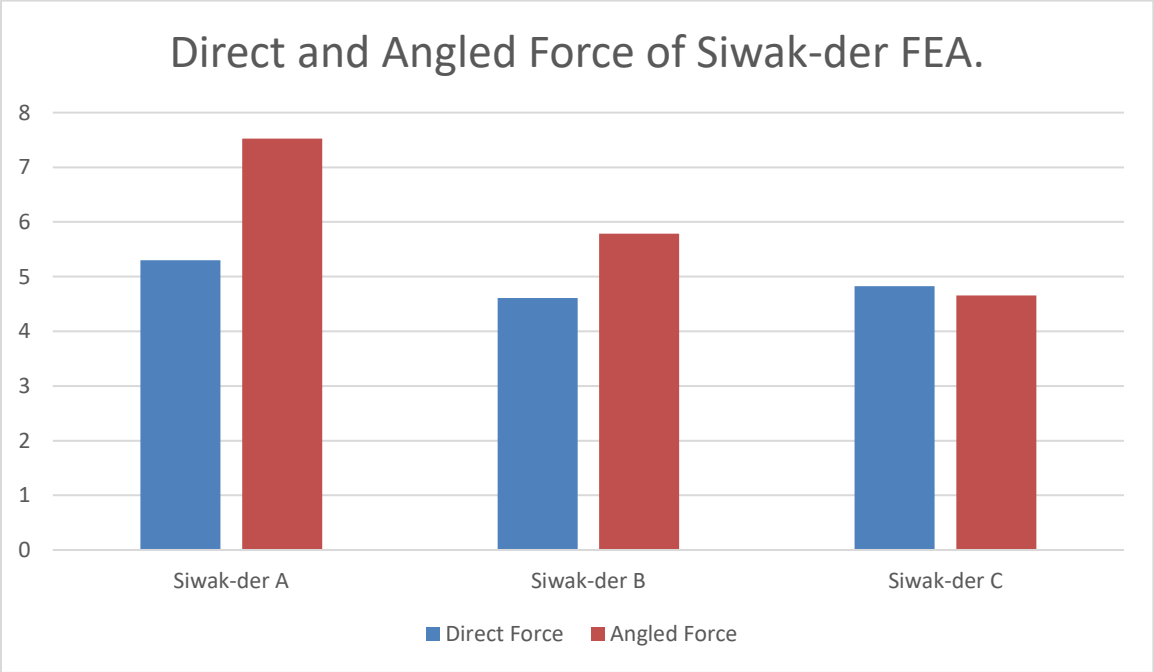

Chart 1 Direct and Angled Force of Siwak-der FEA.

For direct stress, the applied force is increased by a safe factor of 3, increasing the maximum test force from 1.5 N to 5.0 N. For direct stress, 2/3 (Siwak-der 2 and 3) of Siwak-der material reaches a direct stress of less than 5.0 Mpa, i.e. 4.608 Mpa and 4.826 Mpa. It also shows that 2 of the 3 materials (Siwak-der 2 and 3) do not show the effect of the maximum stress marked by a red line on the FEA graph of the Siwak-der in question. Therefore, it can be calculated that Siwak-der 2 and 3 can handle the force required for a toothbrush.

As for the angled force, the applied force is enhanced with a safety factor of 7 by increasing the maximum test force from 0.7 N to 5.0 N. For the angled force, 1 out of 3 (Siwak-der 3) of the Siwak-der material achieves a angled stress of less than 5.0 Mpa which is 4.654 Mpa. It also displays that 1 of the 3 materials (Siwak-der 3) of Siwak-der does not show the effect of maximum stress marked by a red scribble on the FEA graph of Siwak-der in question.

So it can be calculated that Siwak-der 3 is able to handle the force required for a toothbrush. Although 2 out of 3 Siwak-der materials (Siwak-der 1 & 2) exceeded the target of 5.0 Mpa, it should be noted that the study took a high safety factor value of 7 on a scale. Therefore, the Siwak-der 1 & 2 readings that exceed 5.0 Mpa are likely due to the safety factor values that are set somewhat higher than usual. Then there is a possibility that the reading value of Siwak-der 1 & 2 will be less than 5.0 Mpa if the value of the safety factor is set lower than before.

Direct stretching and angled force play an important role in the effectiveness of the toothbrush. While a very strong force in these two types of stress can damage the teeth and gums, a properly controlled force will provide an effective cleaning without harming oral health.

From an environmental sustainability perspective, the use of miswak is gaining traction in the context of the use of everyday ingredients, including oral care products such as miswak and polymer toothbrushes. Following the growing global awareness of the impact of plastics on the environment, miswak is gaining traction as an alternative to toothbrushes made of polymer (plastic) materials. Previous survey studies have also shown a growing interest in the sustainability of miswak, especially since it is more environmentally friendly and renewable. Below is an explanation of the environmental and sustainability issues associated with the use of miswak to replace polymer toothbrushes, as well as their relationship to previous survey studies.

1. Reduction of Plastic Waste

- Polymer toothbrushes made of plastic and nylon have a huge negative impact on the environment, as they are difficult to decompose and contribute to plastic pollution. Discarded toothbrushes often end up in landfills or, worse, in the ocean, where this plastic takes hundreds of years to decompose.
- On the other hand, miswak is a more environmentally friendly natural alternative. Miswak is made from the Salvadora persica tree, which can be regrown and reused without adding a burden to the environment. Miswak, a naturally biodegradable organic material, helps reduce plastic pollution. Abdul wahed et al. (2020)[3] showed that awareness of plastic pollution is pushing more consumers to switch to natural alternatives such as miswak, which are more sustainable and have less negative impact on the environment.

2. Conservation of Miswak Resources

- Miswak springs are natural and renewable. Despite concerns about the destruction of Salvadora persica trees due to overlogging, research shows that the continuous and controlled use of miswak does not cause major damage to the ecosystem. This is in contrast to plastics produced through mining and manufacturing processes, which require a lot of energy resources and continue to have a negative impact on the environment.
- According to a survey study by Al-Maweri et al. (2018)[4], more than 70% of respondents among the Middle Eastern community prefer miswak because it is seen as a more environmentally friendly and sustainable material compared to plastic toothbrushes.

4. Conclusion

Using miswak as a substitute for polymer toothbrushes has great benefits for the environment and is a more sustainable option. Survey studies conducted in various fields show that awareness of plastic pollution and the importance of sustainability are prompting more people to choose miswak as a more environmentally friendly alternative. As a natural and renewable material, Miswak reduces plastic pollution and offers a more sustainable option compared to polymer toothbrushes. Therefore, it is necessary to develop an effort to create a mechanism that supports the use of Miswak. The use of 3D printers in the production of Siwak-der offers several advantages. Not only does it speed up the design process, but it also better adapts to user needs. What's more, 3D printing can reduce material waste, as only essential materials are used during the printing process. The study data also show that polymer materials can be used as a base material in the production of Miswak promoters. However, there are also challenges to face. The initial cost of buying a 3D printer, or the cost of producing a product at scale, can be high for some small entrepreneurs. Therefore, it is necessary to pay attention to efforts to produce Siwak-der products on a large scale. Even more than that, the selection of appropriate printing materials is crucial to ensure the durability and safety of the final product.

References

1. **Zulfikar, M. et al. (2014).** *Chemical Composition and Antibacterial Properties of Miswak: Review*. *International Journal of Pharmacology*.
2. **Mohammad, Z. et al. (2018).** *Antimicrobial Activity of Salvadora Persica (Miswak) Extract Against Oral Pathogens*. *Journal of Clinical Dentistry*.
3. **Abdulwahed, M., et al. (2020).** "Awareness and usage of Miswak in the Middle East: A review." *Environmental Health Perspectives*.
4. **Al-Maweri et al. (2018)**." White oral mucosal lesions among the Yemeni population and their relation to local oral habits."Investig Clin Dent. 2018 May;9(2):e12305. doi: 10.1111/jicd.12305.
5. **Al-Hashmi, S. H., et al. (2004).** "Clinical evaluation of the effectiveness of miswak in oral hygiene maintenance." *Journal of Clinical Periodontology*, 31(7), 528–533.
6. **Morrow, S. (2020).** *The Future of 3D Printing in Medicine: Applications and Innovations*. Journal of Medical Devices.
7. **Pantani, R., et al. (2016).** *Application of 3D Printing Technology in Medicine: Current Developments and Future Perspectives*. Journal of Clinical Medicine.
8. **Gibson, I., Rosen, D., & Stucker, B. (2015).** *Additive Manufacturing Technologies: 3D Printing, Rapid Prototyping, and Direct Digital Manufacturing*. Springer.
9. **Robinson, P. G., Needleman, I. G., & Borrell, R. M. (2005).** "Manual versus powered toothbrushing: A systematic review of the literature." *Journal of Clinical Periodontology*, 32(1), 4-12.
10. **Hyatt, A. A., & Law, D. D. (2009).** "Shear force testing of toothbrush bristles." *Journal of Clinical Dentistry*, 20(2), 60-64.

DETERMINATION OF OPTIMUM T6 HEAT TREATMENT PARAMETERS FOR HOT FORGED AW-4032 ALUMINUM ALLOY PARTS

Mert Karaman[1]

Engineering Chief, Kanca Forging,

mert.karaman@kanca.com.tr

Ömer Batuhan Özkan[2]

R&D Engineer, Kanca Forging,

batuhan.ozkan@kanca.com.tr

Gizem Kocaman[3]

R&D Engineer, Kanca Forging,

gizem.kocaman@kanca.com.tr

Alper Kocakurt[4]

R&D Engineer, Kanca Forging,

alper.kocakurt@kanca.com.tr

Funda Gül Koç[5]

Assist. Assoc. Dr., Kocaeli University, Material and Metallurgical Engineering Faculty
funda.demircan@kocaeli.edu.tr

Ersoy Erişir[6]

Assoc. Prof. Dr. ,Kocaeli University, Material and Metallurgical Engineering Faculty
eerisir@kocaeli.edu.tr

ABSTRACT

Driven by the Green Deal, fuel technologies such as electricity and hydrogen are advancing rapidly. With the increasing volume of electric vehicles in the automotive industry, light metals like aluminum are replacing steel alloys due to demands such as corrosion resistance. Since such parts used especially in the automotive industry are generally used as safety parts, determining the process parameters that will provide the highest mechanical values as a result of the studies will shed light on the aluminum forging and heat treatment industry. Optimizing the heat treatment parameters of aluminum alloys used in hot forged parts is critical to obtain superior mechanical properties after their T6 heat treatment. AW-4032 aluminum alloy, commonly used for automotive parts in as-cast condition, has been the focus of recent research for improving strength of hot forged parts through T6 heat treatment. This study investigates the influence of heat treatment parameters on the mechanical properties and microstructure of an AW-4032 aluminum alloy for hot forged scroll part. Prior to experimental work, forging die design and numerical simulation studies were performed. Following T6 heat treatment, microstructural characterization and mechanical testing were done. The effects of solution annealing temperatures and aging durations on the microstructure and mechanical properties were examined. According to the results, T6 heat treatment following hot forging resulted in an intermetallic morphology of spherical and rod-shaped forms. EDS analysis showed that Fe-free intermetallics were rich in Si, Ni, and Cu, whereas Fe-containing intermetallics exhibited high Ni and Cu but significantly lower Si. Optimum T6 heat

treatment parameters were determined as 510 °C/3h solution annealing +175 °C/6 h aging for AW-4032 quality aluminum forgings.

Key words: AW-4032 aluminum alloy, forging, T6 heat treatment

1.INTRODUCTION

The forging of aluminum alloys, particularly for complex parts like scrolls, plays a critical role in achieving the precise geometries and enhanced mechanical properties needed in high-stress automotive applications. While casting allows for cost-effective production and near-net shaping, it is often insufficient for parts with intricate shapes or demanding performance criteria. Therefore, forging is applied to cast aluminum alloys such as AW-4032 alloy to achieve a denser microstructure and refine grain size, which enhances mechanical properties. For parts like scrolls, which feature complex internal geometries like wraps, close-die hot forging improves material utilization rate and mechanical performance (Cecchel, S., et al., 2020; Zong, Y.Y., et al, 2014)

Aluminum alloys, widely recognized for their strength-to-weight ratio, are replacing steel to meet these demands. To increase their mechanical properties, heat treatments such as the T6 process—comprising solution annealing and aging—are crucial. Recent studies emphasize the need for optimized heat treatment conditions to achieve superior performance. For instance, Ceccel et al. (2020) demonstrated that although both T5 and T6 heat treatments on AW-6082 alloy improved mechanical properties, T5 provided a cost-effective solution with a thinner recrystallized area, making it favorable for certain applications.

In addition to heat treatment, advancements in forging processes have been shown to improve the properties of aluminum components. Zong et al. (2014) applied flow-controlled forging (FCF) to scroll plates, increasing strength by 26% and hardness by 46%, emphasizing the role of controlled back pressure. Hot deformation characteristics of the 4032 alloy were further examined by Zong et al. (2011), who identified optimal forging temperatures (410–450 °C) for minimizing flow stress, which is essential for reliable mechanical performance in automotive applications. Dwivedi et al (2006), are investigated the effect of silicon content and solution and aging temperature on the microstructure, mechanical properties and fracture mode of as-cast Al–(4–20)Si–0.3Mg alloys. Increasing the solution temperature from 450°C to 550°C and aging temperature from 150°C to 230°C increased the tensile strength of all Al–Si–Mg alloys.

As a result of the research conducted on the production methods of AW-4032 type aluminum alloy, Tian et al. (2024), to investigate the issues of coarse microstructure and non-optimal properties in conventional cast 4032 alloys, a dual deformation process including forward extrusion and rotary extrusion (FRE) was used in 4032 aluminum alloys. The findings reveal that the FRE process significantly improves the microstructure of 4032 aluminum alloy, resulting in a more uniform microstructure with less porosity. Barekar et al (2022), describe the first trial of Al-Ni-B addition and its effect on full-scale production, structure and properties of extruded AA4032 products with and without billet homogenization. It was observed that non-homogenized samples performed better during processing and tensile testing compared to homogenized samples.

Other studies on 4032 alloy have reported the impact of process conditions on microstructure and mechanical properties. Lima et al. (2023) demonstrated that recycled 4032 alloy can yield mechanical properties comparable to commercial alloys, providing a sustainable approach with practical application advantages. In addition, mechanical properties can be improved by

methods such as aging. The mechanical values of the forged and heat-treated sample have similar results to the mechanical values of the rolled and heat-treated sample. The open forging process is more efficient due to its easier application. Hu et al. (2011) investigated the effects of process parameters on mechanical properties and microstructure in extrusion production. Wogaso et al. (2021) highlighted that the friction characteristics of 4032 alloy depend on both material surface roughness and lubricant type, with palm oil yielding optimal results through reduced load and enhanced metal flow. Additionally, Balducci et al. (2017) observed that long-term thermal exposure affects aging characteristics of AW-4032 alloys, with peak aging temperatures enhancing hardness. However, prolonged exposure reduces strength and causes over aging. Cahyo et al. (2019) further noted that heat treatment of AW-4032 alloys can significantly improve corrosion resistance, with quenched and artificially aged samples showing superior durability in corrosive environments.

This study investigates the influence of solution annealing temperatures and aging durations in the T6 process for AW-4032 aluminum alloy applied to hot-forged scroll parts. Through optimized T6 parameters, we aim to enhance mechanical properties and microstructure, guiding the industry toward producing sustainable, high-performance aluminum forgings for the automotive sector.

2. MATERIAL AND METHODS

2.1. Design, Simulation and Forging Experiments

The chemical composition of AW-4032 aluminum alloy given detailed in Table 1 conforming to the TS EN 573-3 standard, meets the requirements for both the parts to be produced and the specific customer specifications. The raw material is machined from cast from Ø65 stock and prepared in appropriate dimensions to optimize the forging process.

Table 1. Chemical composition of raw material (wt.%)

	Si	Fe	Cu	Mg	Cr	Ni	Al
Raw Material	12.5	0.33	0.84	0.68	-	0.93	Balance
TS EN 573-3 Standard	11.0-13.5	≤ 1.0	0.5-1.3	0.8-1.3	≤ 0.1	0.5-1.3	Balance

Among the existing forging machine types, hammer presses are not deemed suitable for aluminum materials because they provide rapid shape changes, and this will cause quality defects on the material. For this reason, a crank press machine was used, and a 2500-ton press was considered suitable by calculating the minimum force required to shape the part. In Fig 1, forged model of scroll part was created in accordance with general forging design rules and by adhering to customer technical drawings. The burr line transition point of the part, the draft angles that will allow easy separation from the die and the radius that will not create quality problems in the forging process design were optimized. Part technical drawing tolerances were determined according to TS EN 586-3 standard.

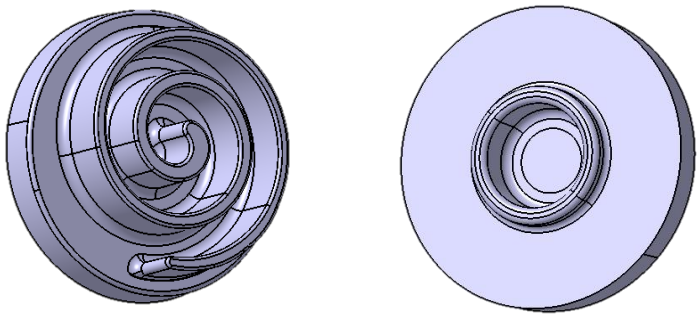

Figure 1. Forged part model.

Due to the difficulty of forming the scroll part on the die design and process design side, any preliminary draft operation was not considered appropriate, and the final shape was forged directly as shown in Fig 2. Since the part will cool down with each additional preliminary draft operation, it would be difficult to create the final form properly. A 10-ejector die system was designed because the deep engraving structure of the part would cause difficulties in sticking to the die and production.

In the selection of die steel, 1.2343 quality hot work tool steel was used, based on the raw material, shape (deep engraving) of forged parts and the type of machine used.

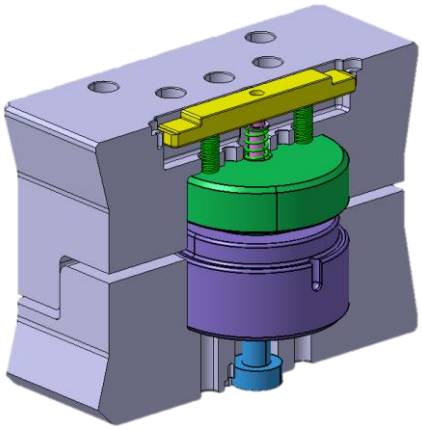

Figure 2. Forging die design images

The ideal temperature range for the part was determined theoretically between 400-500 ºC. Hot forging simulation studies were conducted to determine i) the accuracy of these parameters determined before forging production, ii) the weight of the raw material, iii) the press force of the part and iv) possible defects. According to the simulation results, the hot forging parameters are determined. It is observed that the minimum requirement for press force is 1620 tons and no hot forging defect is encountered as shown in Fig 3.

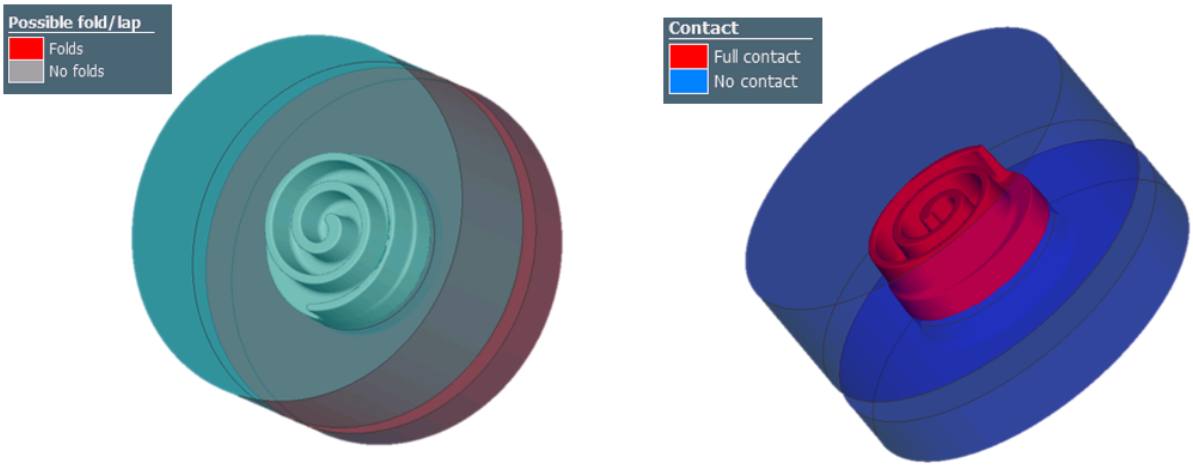

Figure 3. Simulation results images

An electric furnace was used for raw material pre-heating and in parallel with the simulation results, the ideal temperature range of 400-500 ºC was correctly determined. During the hot forging, the parts coming out of the furnace were measured with a pyrometer. The hot forging was started after the correct temperature was reached. As a result of the preliminary studies and evaluations, the part was manufactured without any problems and defects.

2.2. Heat Treatment and Hardness

The T6 heat treatment of aluminum alloys includes a three-step process of solution annealing, quenching, and aging. During solution annealing and quenching, the alloy is rapidly cooled from solution annealing temperature to prevent the precipitation of dissolved elements, resulting in a supersaturated solid solution. The final aging step promotes the formation of precipitates, which significantly increases hardness and strength. Literature indicates that optimal microstructure and high mechanical properties for AW-4032 aluminum alloy are achieved with solution annealing at 505–515˚C for 3 hours. For the aging, studies show that aging at 170–175˚C for durations of 6, 8, and 12 hours produces favorable results. To determine the optimum heat treatment conditions, different heat treatments were performed to forged parts. Hardness measurements were made on heat-treated and forged materials under a 3 kg load for 10 seconds. The hardness of forged material was measured as 80 HV. Heat treatment conditions and hardness of the materials given in Table 2.

Table 2. T6 heat treatment parameters of forged AW-4032 material

Sample	Solution Annealing	Aging Parameters	Hardness (HV3)
A1	510 °C / 3 saat	175 °C / 6 saat	128
A2		175 °C / 8 saat	127
B1	530 C / 3 saat	175 °C / 6 saat	138
B2		175 °C / 8 saat	132

3. RESULTS AND DISCUSSION

Samples were taken to examine the microstructure of forged and T6 heat treated materials. The samples were prepared metallographically and they were etched with Keller etchant for 20 seconds to reveal microstructure. Light microscope images of these samples are given in Figure 4 and Figure 5. Microstructural examinations showed that the dendritic structure from the casting still exists in the forged and heat-treated position. It was observed that the matrix structure became more distinct as a result of the increase in the dissolution of the phases in the α-matrix as the solution temperature increased. Also coarsening alpha grains and grain separations was observed in Figure 5.d and Figure 5. e. For this reason, it is thought that the solution process at 530 °C is risky for these alloys.

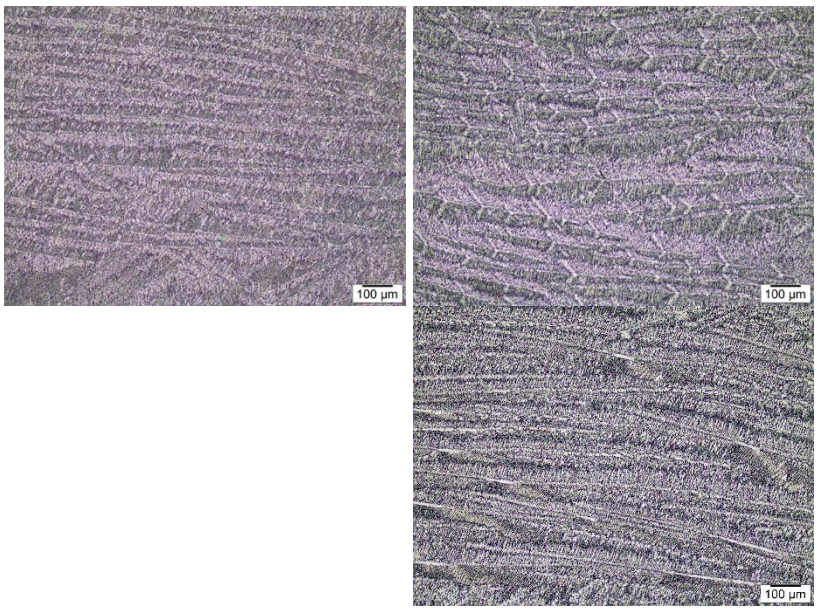

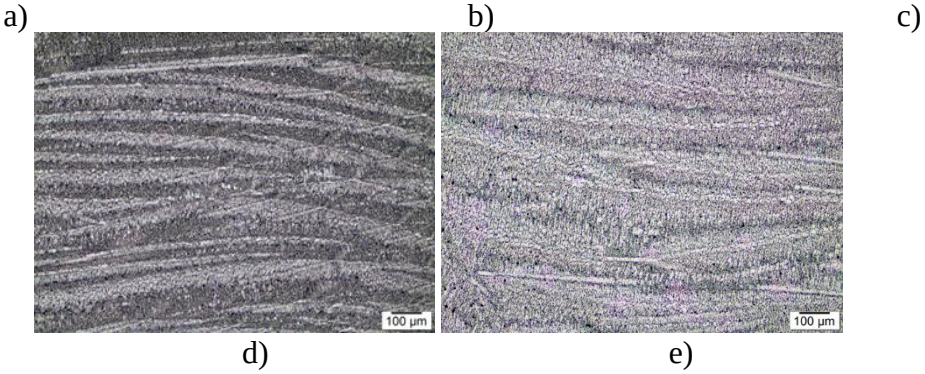

Figure 4. Light microscope images of forged and T6 heat treated materials a) forged condition, b) A1, c) A2, d) B1, e) B2

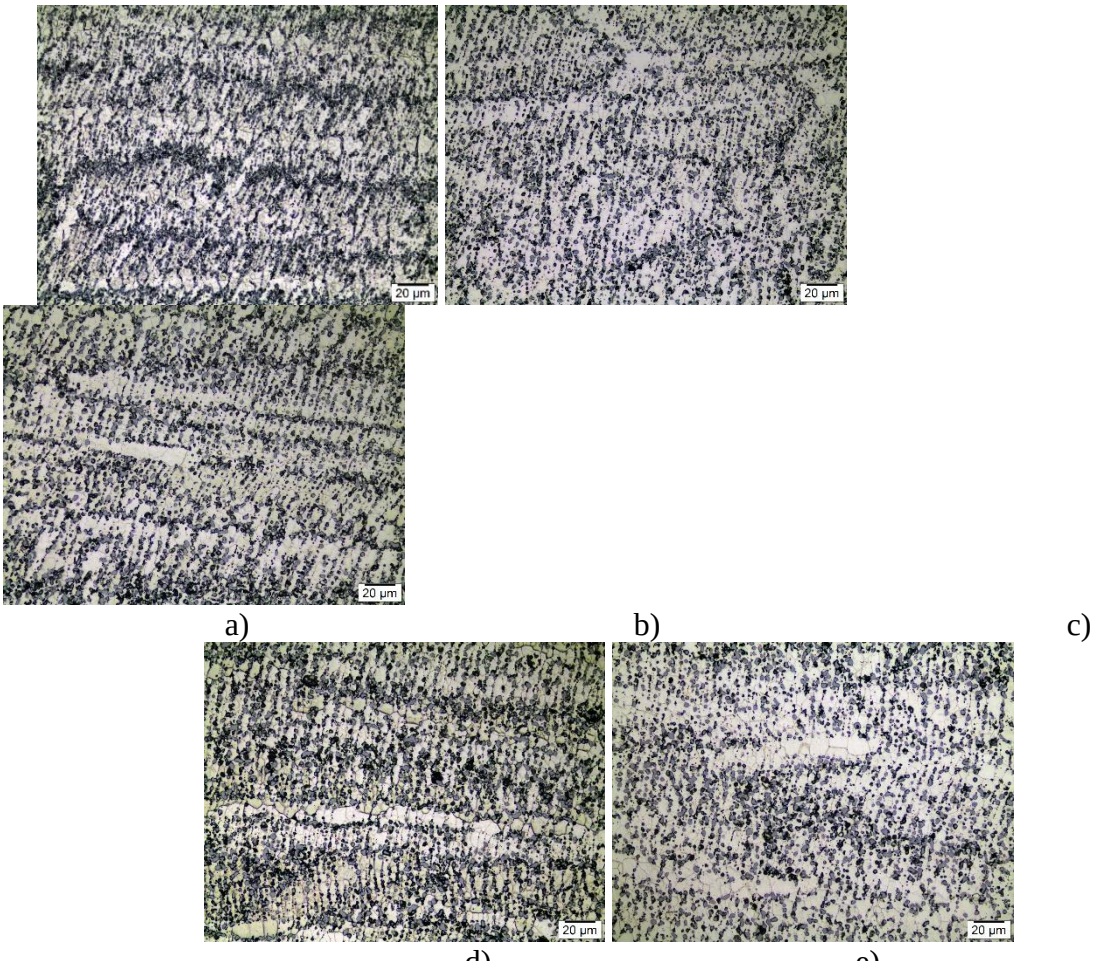

Figure 5. Light microscope images of forged and T6 heat treated materials a) forged condition, b) A1, c) A2, d) B1, e) B2

In order to examine the phases observed in the microstructure in more detail, microstructural characterization studies were carried out using Scanning Electron Microscope (SEM) with EDX (Energy Dispersive Spectroscopy) attachment. In the SEM images given in Figure 6, it was observed that there were homogeneously distributed precipitate phases in the microstructure. With the EDX analyzes given in Figure 7 and Figure 8, it was determined that there were different precipitates containing Si, Cu, Mg, Fe and Ni in the microstructure. Compared to the intermetallic phases found in as-cast and as-deformed conditions reported in the literature [4,8], the typical needle-like morphology of intermetallics was not observed in

this study (Figs. 7 and 8). Instead, more spherical and rod-shaped precipitates were present, likely resulting from the T6 heat treatment applied after hot forging. The intermetallics in Fig. 7 contain substantial amounts of Si (5.6–25.5%), Ni (8.5–17%), and Cu (3.0–5.5%), with trace amounts of Mg (0.5–0.8%) and no detectable Fe. In contrast, Fig. 8 shows Fe-containing intermetallics with significant levels of Ni (11.9–13.4%) and Cu (6.4–8.7%), as well as Fe (0.9–1.7%). Although the Ni and Cu contents are similar between Fe-free and Fe-containing intermetallics, the latter exhibits much lower silicon concentrations (1.8–3.5%).

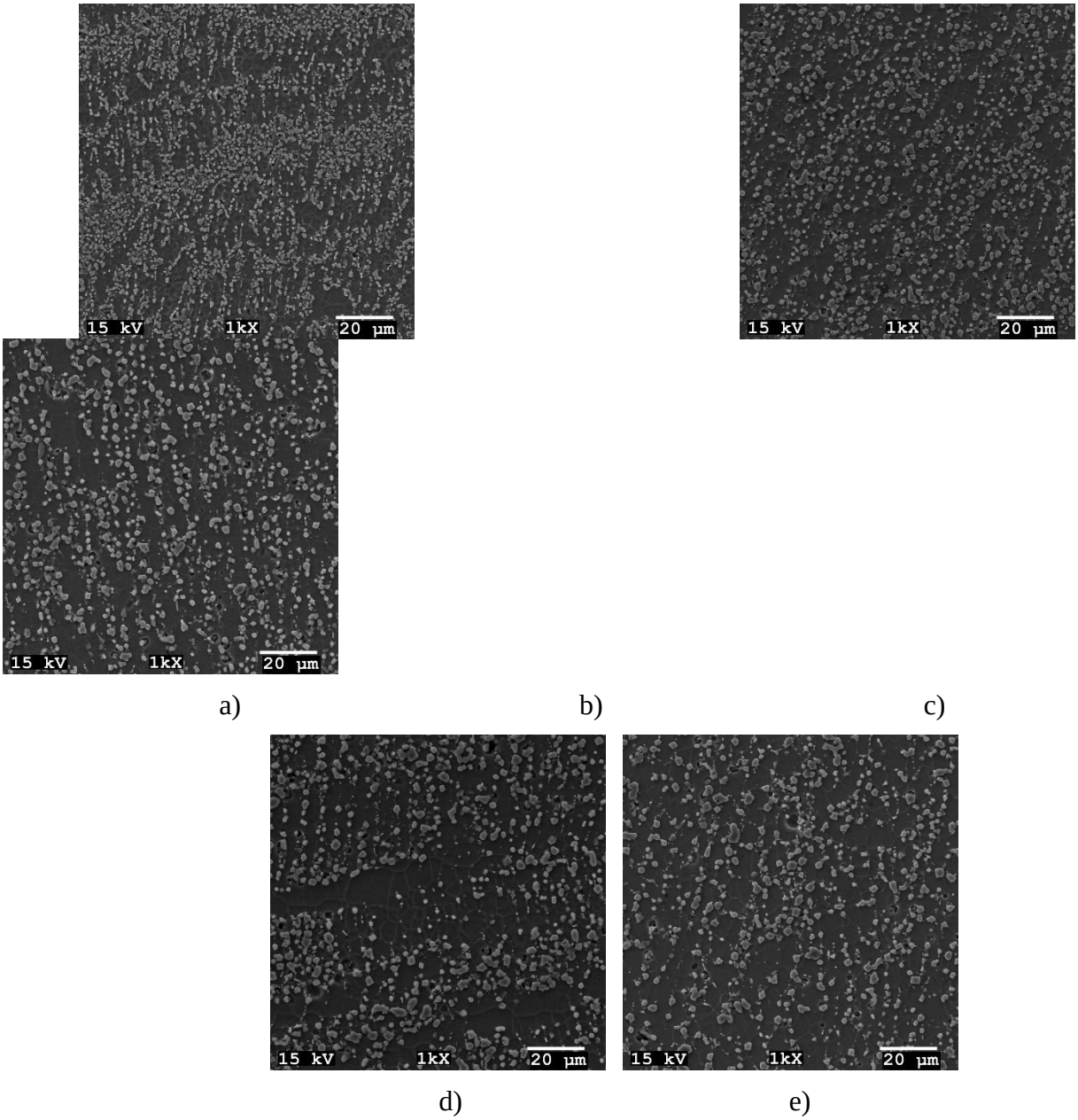

Figure 6. SEM image of forged and heat treated AW-4032 materials a) forged condition, b) A1, c)A2, d) B1, e) B2

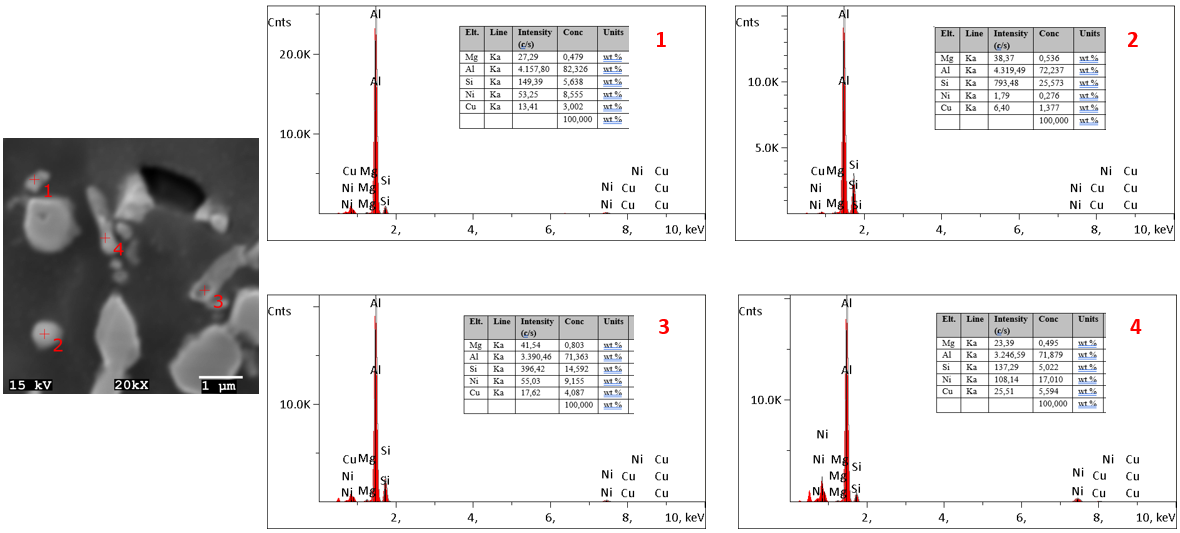

Figure 7. SEM image and EDX analysis of forged AW-4032 material

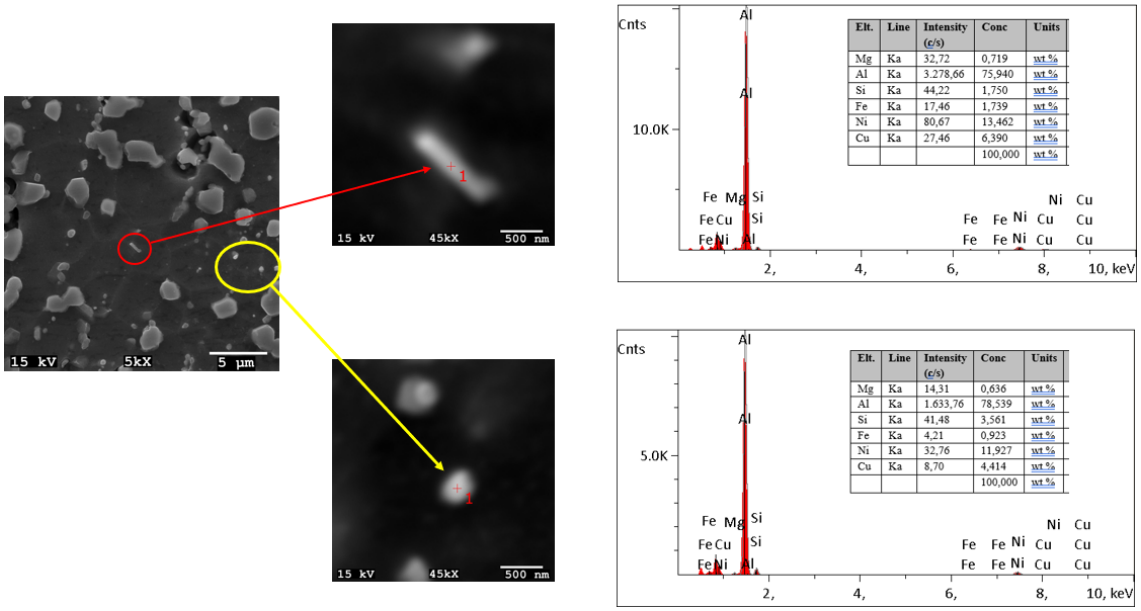

Figure 8. SEM image and EDX analysis of sample A1

4. CONCLUSION

Within the scope of this study, T6 heat treatment was applied at different parameters after the die design, simulation and forging production of the Scroll part to be produced from AW-4032 quality aluminum alloy. The results obtained from the experiments and studies are shown below;

- Scroll part was produced in crank type press with AW-4032 quality raw material as forging. AW-4032 quality raw material was heated between 400-500º C. Electric furnace was used to heat the raw material. The press force required to form the scroll part was determined as 1620 tons by simulation studies. After the forging tests, it was determined that the press force determined in reality, and the simulation value were the same.

- The temperature of solution annealing of aluminum which is 530˚C was deemed risky because it causes regional grain separation, alpha grains become coarser and evident, diminishing silicon.

- Hot forging and following T6 heat treatment significantly influences the morphology of intermetallic phases. Unlike the typical needle-like intermetallics often observed in as-cast and as-deformed conditions according to literature, more spherical and rod-shaped precipitates were found. Two types of intermetallics were observed as a) Fe-free intermetallics rich in Si (5.6–25.5%), Ni (8.5–17%), and Cu (3.0–5.5%) with low Mg content and b) Fe-containing intermetallics which have high Ni (11.9–13.4%) and Cu (6.4–8.7%) but lower Si levels (1.8–3.5%). While the hardness of the material after forging was 80 HV, the hardness of the material increased by an average of 65% with T6 heat treatment. T6 heat treatment parameters that provided proper microstructure and provide high mechanical properties at different temperatures and times were determined as 510˚C/3 hours and 175˚C/6 hours.

References

[1] Cecchel, S., Ferrario, D., & Cornacchia, G. (2020). Heat treatments of EN AW 6082 aluminum forging alloy: effect on microstructure and mechanical properties. *International Journal of the Italian Association for Metallurgy.*

[2] Zong, Y.Y., Chen, L., Zhao, Z.G., & Shan, D.B. (2014). Flow lines, microstructure, and mechanical properties of flow control formed 4032 aluminum alloy. *Materials and Manufactoring Processes.*

[3] Zong, Y.Y., Shan, D.B., & Shi, Z. (2011). Study on hot deformation behaviour and constitutive equation of 4032 Al alloy. *Materials Research Innovations.*

[4] Lima, J.I.V., Pastor, F.A.G., & Valdés, A.F. (2023). The Effect of Heat Treating and Deformation by Rolling and Forging on the Mechanical Properties of the 4032-Type Alloy Prepared from Recycled Materials. *Metals*.

[5] Wogaso, D., & Hamda, M. (2021). Studies on friction behaviour of aluminium AA4032 alloy during forging using ring compression test. *International Journal of Engineering.*

[6] Balducci, E., Ceschini, L., Morri, A., & Morri, A. (2017). En Aw-4032 T6 piston alloy after high-temperature exposure: residual strength and microstructural features. *Springer.*

[7] Cahyo, F.N., & Soegijono, B. (2019). Effect of solution heat treatment of aluminum alloy 4032 on the structure and corrosion resistance in 3,5% and 10,5% NaCl solution. *IOP Conference Series: Materials Science and Engineering.*

[8] Barekar, N.S., Skalicky, I., Wang, S., Shurkin, P., Adole, O., Babu, N.H., & Jarrett, M. (2022). Comparative Analysis of Structure and Properties of Nb-B Inoculated Direct Chill Cast AA4032 Alloy Extruded from As-Cast and Homogenized Conditions. *JOM.*

[9] Tian, H., Zhao, X., Ma, D., Meng, J., Li, H., Liu, X., Zhao, G., Zhang, G., Zhao, R., & Wu, F. (2024). Effect of Double Deformation Extrusion on the Microstructure and Properties of 4032 Aluminum Alloy. *SSRN.*

[10] Dwivedi, D.K., Sharma, R., & Kumar, A. (2006). Influence of silicon content and heat treatment parameters on mechanical properties of cast Al-Si-Mg alloys. *International Journal of Cast Metals Research.*

[11] Hu, H., Kong, X., Shao, Z., & Wang, X. (2011). Thermoplastic deformation behaviour of 4032 Al alloy. *Scientific.*

3 BOYUTLU STEROTİGRAFİ YAZICILARDA KULLANILAN REÇİNENİN KATKI MALZMELERİ İLE GELİŞTİRİLEREK DÜŞÜK BASINÇLI PLASTİK ENJEKSİYON CİHAZLARINDA PROTOTİP ÜRÜN KALIBI ÜRETİMİNE UYGUN DAYANIMDA KULLANILABİLECEK BİR REÇİNENİN ARAŞTIRILMASI VE UYGULANMASI

Emre ÇİFTÇİ[1], Renç ELDENER[2]

[1]Desird Tasarım Arge Anonim Şirketi, emrec@desird.com
[2]Desird Tasarım Arge Anonim Şirketi, renceldener@desird.com

Özet

Prototipleme ve seri üretim öncesi numune ürün üretimi, Ar-Ge sürecinin önemli bir parçasıdır. Elektronik kartların ve kabloların plastik granüllü enjeksiyon yöntemiyle kaplanması bu süreçlerden bir tanesidir. Elektronik kartların enjeksiyon sürecinden zarar görmemesi adına işlemin düşük basınç ve sıcaklıkta gerçekleşmesi gerekmektedir. Bu iş için özelleşmiş enjeksiyon malzemesi ve makinesi kullanılması zaruridir. Bu amaçla kullanılan cihazlara "Düşük Basınçlı Enjeksiyon Cihazı" adı verilir ve bahsedilen süreçlerde yaygın olarak kullanılır. Bu cihazlarda kullanılan kalıpların tasarımı ve üretimi nispeten yüksek maliyetlidir. Prototipleme sürecinde her bir deneme için ayrı metal kalıp tasarlanması, üretilmesi ve uygulamaya alınması; zaman, maliyet ve iş gücü açısından yüksek isterlere sahiptir. Bu çalışma kapsamında, tasarım sırasındaki kalıp maliyetini düşürmek amacıyla üç boyutlu yazıcı sistemlerinden biri olan SLA (Stereolitografi) yazıcıların kullanabileceği öngörülmüş ve prototip kalıp üretimine uygun bir reçine geliştirilmiştir. Piyasada halihazırda var olan reçineler kullanılarak elde edilen SLA baskı sonucunda çıkan ürünlerin ısıl ve fiziksel dayanımı, düşük basınçlı plastik enjeksiyon işlemi için yeterli olmadığı görülmüştür. Bu çalışmada ise geliştirilen reçine içine belirli oranlarda farklı katkı malzemeleri karıştırılarak, hedef isterleri karşılayabilecek bir ürünün elde edilmesi üzerine çalışılmıştır. Çalışma sonucunda elektronik kartlara zarar vermeden, yüksek yüzey kalitesine ve dayanıma sahip, kalıplamaya uygun bir reçine türü geliştirilmiştir. Bu kapsamda özellikle prototip çalışmaları için çoklu kullanıma uygun bu ürün sayesinde; büyük ölçüde zaman, maliyet ve iş gücü kazanımı sağlanabilecektir.

Anahtar kelimeler: Düşük basınçlı plastik enjeksiyon, SLA yazıcı, reçine, prototip kalıplama

Abstract

Prototyping and pre-serial production sample product production is an important part of the R&D process. Coating of electronic cards and cables with plastic granule conversion method is one of these processes. In order to reduce the damage during the processing of electronic cards, the process must be increased and increased at low pressures. It is essential to use customized regulation material and machine for this job. The devices used for this purpose are called "Low Pressure Injection Device" and are widely used in use. The design and production processes of the molds used in this product are used at a high rate. Separate metal mold design, features and implementation for each trial in the prototyping process have high demands in terms of time, cost and labor. Within the scope of this study, in order to reduce the mold cost during design, SLA (Stereolithography) printers, one of the three-dimensional printer systems, can be presented and a resin suitable for prototype mold production was

produced. The poor thermal and physical performances resulting from SLA printing obtained with existing resins registered in the market were not sufficient for low-temperature plastic processing process. If this is soluble, it is achieved by mixing different additives in certain proportions to obtain a product that can be met for the target. As a result of the study, there is a resin type suitable for molding, with a loss of damage to electronic cards, high surface quality and durability. Thanks to this ability, this product, which is suitable for multiple use especially for prototype studies; It will be possible to obtain a large amount of time, cost and labor.

Keywords: Low Pressure Plastic Injection, SLA Printer, Prototype Molding

1. GİRİŞ

Eklemeli imalat her geçen gün gelişmekte olan bir teknolojidir. Farklı kullanım alanları için farklı malzemelerin kullanıldığı, farklı özelliklere sahip flament ve reçineler geliştirilmekte, bu reçinelerle uyumlu yeni yazıcılar geliştirilmektedir. Eklemeli imalat teknolojisi ile özellikle üretim sektörünün farklı alanlarındaki uzun ve maliyeti yüksek süreçlerin kolaylaştırılması ve bu parametrelerde iyileştirilmiş sonuçlar alınması mümkün kılınmıştır.

Bahsi geçen geleneksel üretim süreçlerine kalıplama dahil edilebilir. Kalıplama süreci enjeksiyon işleminin olmazsa olmaz bir parçasıdır. Enjekte edilecek malzemenin talep edilen hacim ve ölçülerde olabilmesi için detaylı bir kalıplama prosesinden geçmesi gerekmektedir. Kalıp üretme süreci meşakkatli ve yüksek maliyetlidir. Bahsi geçen süreç yüksek sıcaklık ve basınç dayanımına sahip malzemelerin (genellikle metallerin) enjeksiyon süreci ve kanalları göz önünde bulundurularak işlenmesi ve montajını içerir. Kalıp maliyetleri bu nedenle oldukça yüksektir ve bir kalıbın kullanıma hazır hale gelebilmesi genellikle fazla zaman almaktadır. Eklemeli imalat prosesinin bu alana dahil edilebilmesi için yüksek ısı ve basınç isterlerini karşılayabilecek ve aynı zamanda yüksek hassasiyette basım gerçekleşebilecek malzeme SLA (Stereolitografi) reçinedir. SLA yazıcılar, genellikle flamentlli yazıcılara göre çok daha küçük toleranslarda baskı yapabilmektedirler. Ayrıca malzemenin yapısı gereği flament malzemelere göre daha yüksek ısı ve basınç dayanımına sahiptir. Bu nedenle özellikle enjeksiyon kalıplarında kullanılmak üzere SLA reçine güçlendirici katkı malzemeleri üzerine çalışmalar gerçekleştirilmiştir [1-2].

SLA reçineli 3 boyutlu yazıcılarında UV kürleme süreci bulunmaktadır. Cihazın alt yüzeyinde bulunan LCD ekrana basılması istenilen tasarımın görüntüsü uygun ışık aralığında verilir. Böylece tasarıma ait katmanlar reçinenin kürlenmesi ile katılaşır ve tasarım yazdırılır. Ardından basılan tasarımın izopropil alkol ile temizlenmesi ve son kez kürlenme süreci gerçekleşerek baskı süreci tamamlanır. SLA reçinede UV kürlenme oldukça kritik olduğu için, reçineyi güçlendirecek katkı malzemelerinin de aynı şekilde UV ışıkla kürlenebilir yapıda bulunması gerekmektedir. Bu konu ile ilgili yapılan araştırmalarda sektörde Silica temelli malzemelerin, katkı malzemesi olarak kullanıldığı görülmüştür [3]. Silica temelli malzemelerin yanı sıra ayrıca POSS (Polihedral Oligomerik Silseskioksan) katkılı nanokompozitlerin de ısıl ve mekanik dayanımını arttırdığı üzerine çalışmalar bulunmaktadır [4-5].

Elektronik sektöründe, elektronik kartlara uygulanan enjeksiyon malzemesi genellikle plastiktir. Yüksek ısı ve yüksek basınç değerlerinde enjeksiyon işlemi gerçekleştirilemez. Çünkü elektronik kartların üzerinde bulunan devre elemanlarının mekanik ve ısıl dayanımları nispeten düşüktür. Bu isterleri karşılayabilmek adına “Düşük Basınçlı Enjeksiyon Cihazları” kullanılır. Sıcak enjeksiyon malzemesi çok düşük bir basınç değeri ile (0, 15 MPa – 4 MPa)

kalıba enjekte edilir. Enjekte edilen plastik çok hızlı bir şekilde soğur ve kullanıma direkt hazırdır. Bu nedenlerle elektronik sektöründe düşük basınçlı enjeksiyon cihazlarının kullanımı tercih edilmektedir. Ayrıca düşük basınçlı sistemle prototip ürünler üzerinde çalışmak düşük maliyeti ve hızlı sonuçlar elde edilebilmesi nedeniyle akılcıdır.

Düşük basınçlı ve düşük sıcaklı sistemler olmasına rağmen halihazırda SLA reçineleri ile çalışmak için uygun değillerdir. Yapılan çalışmalarda SLA reçine baskısı kalıpların, düşük basınçlı enjeksiyon sistemlerinde sızdırmalara, şekil değişikliklerine ve yüzey kalitesinde bozulmalara neden olduğu görülmüştür. Yapılan araştırmalarda ise bu sistemlerle uyumlu şekilde çalışma gerçekleştirilebilecek doğrudan bu amaçla kullanıma uygun bir reçine görülmemiş ve sürecin avantajlarının değerlendirilebilmesi adına konu ile ilgili Ar-Ge çalışmalarının yapılması kararlaştırılmıştır.

2. MALZEME VE YÖNTEM

Eklemeli imalat teknolojisinin en eski metodu olan SLA hala günümüzde en çok tercih edilen eklemeli imalat teknolojisidir. Alternatiflerine göre yüksek yüzey kalitesi, hızlı baskı yapabilmesi, yüksek hassasiyet gibi avantajları bulunmaktadır. Reçine, işleme tabi olmadan önce sıvı yüksek viskoziteye sahip bir sıvıyken, ultraviyole ışık ile kürlenerek sert plastik dokusu kazandırılır. 3 Boyutlu yazıcıda tercih edilen teknolojiye göre bahsi geçen UV ışık kaynağı (DLP, LCD) değişiklik gösterebilmektedir. SLA reçineleri termoset polimerlerden oluştuğu için bir kere kürlenen bir reçinenin tekrar kürlenmeden önceki sıvı hali kazandırılması mümkün değildir.

SLA reçinelere ikincil malzemeler eklenerek reçinenin fiziksel özelliklerinde değişiklik yapılabilir. Buna örnek olarak seramik ve cam eklenmesi ile ısıl dayanımında ve darbe mukavemetinde artış sağlanması verilebilir.

Yapılan akademik araştırmalar sonucunda silica, grafit, elyaf gibi katkı malzemelerinin SLA reçineye ait fiziksel özelliklerde artırılmış dayanım sağladığı görülmüştür. Bu nedenle Silica ve grafit tedarik edilerek bir deney planı hazırlanmıştır.

Deney sırasında kullanılan ELEGOO firmasının ürettiği Saturn 3 model yazıcı ile Anycubic firmasının üretmiş olduğu Standart Beyaz reçine Şekil 1'de gösterilmiştir.

Şekil 1. Baskı almak için kullanılan 3D yazıcı ve sıvı reçine

Üretilen numunelere basınç (kırılma), sertlik ve ısı testi yapabilmek amacıyla 15x15x70mm ölçülerinde parça tasarımı yapılmıştır. Parça çizimini yazıcıya aktarma işlemlerinde Şekil 2 de örneği görülen "Chitubox Basic" yazılımı kullanılmıştır.

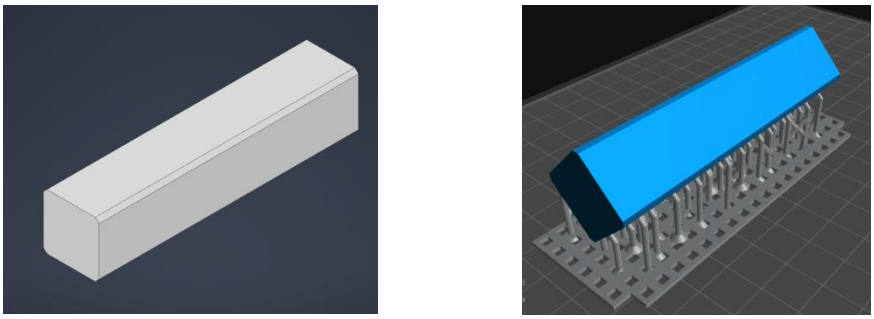

Şekil 2. Test parçası ve SLA baskı şekli

Öncelikle bu malzemelerin homojen olarak karışması ve UV ışık ile kürlenebilir olması süreç için oldukça kritik bir öneme sahiptir. Bu nedenle baskı öncesi belirlenen oranlarda karışım yapıldıktan sonra 5 dakika boyunca reçine homojen hala gelene kadar karıştırıldıktan sonra üretilen numuneler 2.5 s bekleme süresi ile her basamakta 50 µm katman kalınlığı olacak şekilde baskı alınmıştır. Ayrıca baskı alınırken parçanın düzgün bir şekilde çıkması için 45° derece açı ile destek kullanılmış ve %100 doluluk seviyesi uygulanmıştır. Son olarak çıkan numuneler izopropil alkol ile yıkandıktan sonra 395-400 nm dalga boyuna sahip bir UV LED lamba altında 5 dakika süreyle kürlenmiştir.

Deney sırasında UV rezine ek olarak farklı oranlarda Küresel 99.95+%13-22 nm Nanogözenekli ve Amorf S-tipi Silikon Dioksit Nano Tozu ve SC80 25 Mikron Grafit Tozu kullanılmıştır.

Deney için Desird Alakart V1.1. kartı döküm sırasında kaplama amacıyla kullanılmıştır. Ayrıca kartın kaplanması için ise Werner Wirth firmasının üretmiş olduğu Şekil 4'te görülen TM2000 model Düşük Basınçlı Plastik Enjeksiyon cihazı kullanılmıştır. Kartın üzerine dolgu malzemesi olarak ise Bostik firmasının elektronik kart kaplama için ürettiği Thermelt T4229 dolgu malzemesi kullanılmıştır.

Şekil 4. Test için kaplama yapılan Devre kartı ve düşük basınçlı plastik enjeksiyon cihazı

Son olarak döküm işlemlerinin gerçekleştirmek amacı ile Şekil 5'teki kart kalıbı tasarlanmış ve bu kalıplar ile elektronik devre kartı olan "Alakart" içerisine yerleştirilerek döküm denemeleri yapılabilir hale getirilmiştir

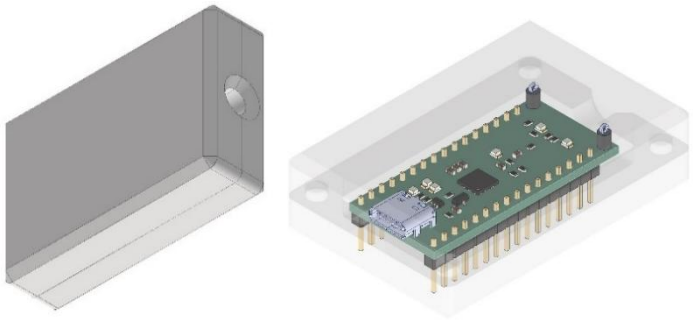

Şekil 5. Kart kalıbı tasarımı

3. BULGULAR

Deney sırasında standart reçine içerisine farklı karışım oranlarında Silikon Dioksit ve Grafit Tozu kullanılmıştır. Temel olarak Silikon Dioksit kullanım amacı kalıbın çoklu baskı dayanımını artırmak iken Grafit Tozu kullanarak ise ısıl dayanımı ve yüzey kalitesinin iyileştirilmesi hedeflenmiştir. Bu amaçla elde edilen karışımlar ile öncelikli olarak Şekil 6'daki test parçaları basılmış ve yine aynı şekilde bu parçaların basınç altında kırılma dayanımları test düzeneğinde denenmiştir.

Şekil 6. Test parçaları ve basınç altında kırılma test düzeneği

Ardından, yine aynı parçalar Şekil 7'deki gibi oda sıcaklığında ve Düşük Basınçlı Plastik Enjeksiyon cihazının çalışma sıcaklığı olan 200 C° sıcaklıkta Shore-D sertlik testine sokulmuştur. Son olarak ise elde edilen baskıların yüzey kalitesi değerlendirilmiştir.

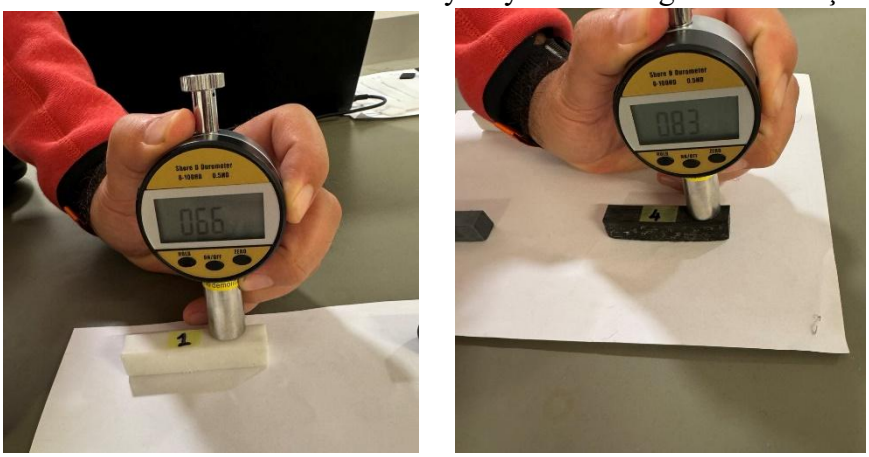

Şekil 7. Shore-D sertlik testi

Bu testler sonucunda elde edilen sonuçlar Tablo 1' de değerlendirilmiştir. Farklı karışım oranları ve standart reçine kıyaslandığında ilgili tabloda da görüleceği gibi 3 numaralı karışım oranı denemeler sonucunda deneyin amacına en ideal karışım oranı olarak görülmektedir.

Tablo 1. Karışım oranları

#	Kullanılan Materyel	24 °C Shore D (HD)	200 °C Shore D (HD)	Maksimum Kırılma Basıncı (N)	Yüzey Kalitesi
1	%100 Anycubic Standart Beyaz Reçine	0.66	0.58	204	Orta
2	%98 Anycubic Standart Beyaz Reçine %1 Silikon Dioksit Nano Tozu %1 SC80 25 Mikron Grafit Tozu	0.7	0.64	217	Orta
3	%97 Anycubic Standart Beyaz Reçine %1 Silikon Dioksit Nano Tozu %2 SC80 25 Mikron Grafit Tozu	0.755	0.693	263	Yüksek
4	%96 Anycubic Standart Beyaz Reçine %2 Silikon Dioksit Nano Tozu %2 SC80 25 Mikron Grafit Tozu	0.83	0.722	238	Düşük

Bu değerlendirme ışığında tasarlanan kalıp katkısız ve katkılı olarak iki farklı şekilde SLA yazıcı ile üretilmiştir. Şekil 8'de solda katkısız sağda ise 3 numaralı test karışımının basılmış hali görülmektedir.

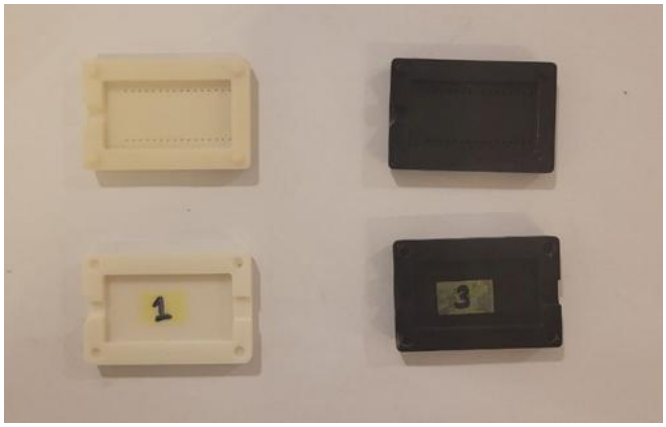

Şekil 8. Katkısız 1 numaralı ve 3 numaralı katkılı kalıp baskısı

Son olarak Düşük Basınçlı Plastik Enjeksiyon cihazı ile bu kalıplara Şekil 9'daki gibi baskılar alınmıştır. Alınan baskılar ile elde edilen çıktılar değerlendirildiğinde kalıptan çıkan döküm yapılmış kartın yüzey kalitesi ve kalıbın 5 baskı sonrası durumu Şekil 10'da görülebilmektedir. Bu görsellerden de anlaşılabileceği gibi çoklu basım sonrası katkılı reçine baskı kalitesini korurken standart reçinede aşınmalar ve istenmeyen durumlar oluşmuştur. Şekil 11'de ise 1 numaralı standart beyaz reçine ile ve 3 numaralı katkılı reçine ile basılmış

kalıpların 5 basım sonrasındaki yüzey kalitesinin mikroskop altındaki görüntüsü paylaşılmıştır.

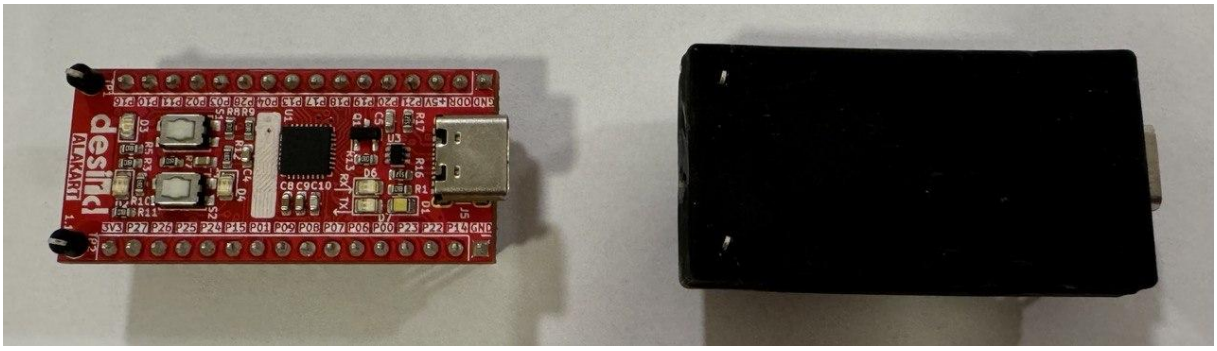

Şekil 9. 3 Numaralı Kalıp ile Basılan Ürün ve Baskısız Kart

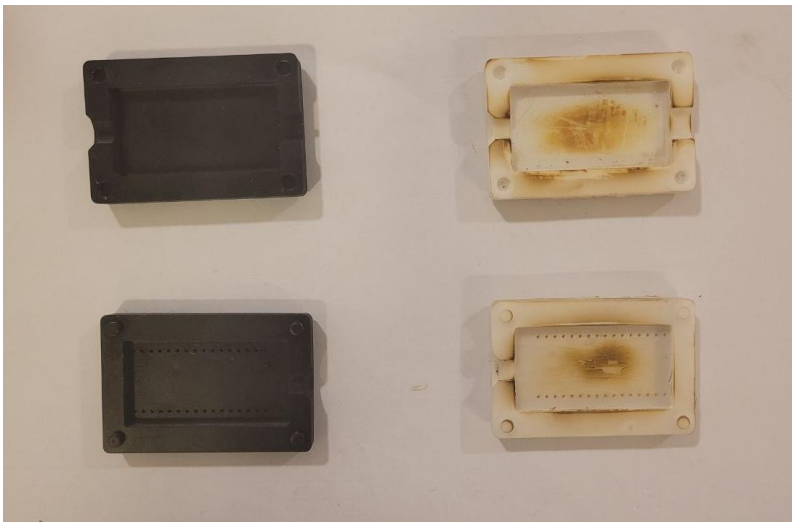

Şekil 10. 5 Basım Sonrası 3 Numaralı ve 1 Numaralı Numunelerle Hazırlanmış Kalıplar

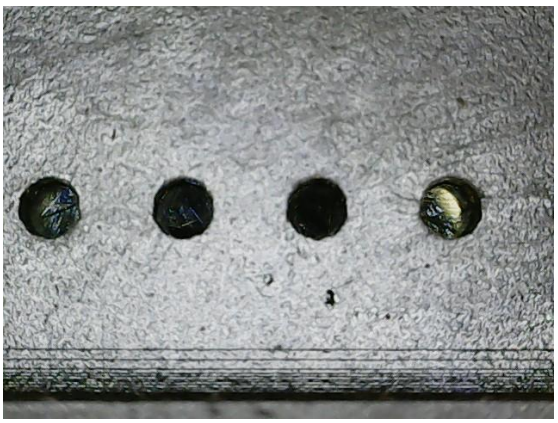

Şekil 11. 1 Numaralı ve 3 Numaralı Numunelerle Hazırlanmış Kalıpların 5 Basım Ardından Mikroskop Altındaki Görünümleri

4. SONUÇ, TARTIŞMA VE ÖNERİLER

Bu çalışmada standart reçine içerisine sadece iki farklı malzeme ekleyerek reçinenin Düşük Basınçlı Plastik Enjeksiyon cihazlarının çoklu baskısı için fayda sağladığı görülmüştür. Kullanılan katkı maddelerin ve standart reçine dışında ABS benzeri reçine gibi farklı reçine tiplerine daha çeşitli katkı materyalleri karıştırılarak mevcut dayanım ve yüzey kalitesi daha da artırılabileceği görülmektedir.

Günümüzde reçine çeşitleri hızla artmaktadır, artık ürün ve uygulama alanına göre çok daha spesifik reçine türleri geliştirilmektedir [6]. Bu çalışma ile hızlı prototiple ihtiyaçlarına çok daha uygun bir reçine karışımı geliştirilmiş ileride de doğrudan üretici firmalardan bu amaçla satışa sunulacak Düşük Basınçlı Plastik Enjeksiyon kalıp reçinesi de bulunması bu ve buna benzer çalışmalar sayesinde olası görülmektedir. Bir diğer alternatif ise mevcut standart reçineler içine sonradan eklenebilir katkı karışımları piyasaya sürülerek her kullanıcı kendi ihtiyacına göre optimum fayda maliyeti sağlayabilir.

5. KAYNAKLAR

[1] Benitez-Lozano A., Vargas-Isaza C., Montealegre-Rubio W., 2023. Development, Simulation of Temperatures, and Experimentation in Injection Molds Obtained through Additive Manufacturing with Photocurable Polymeric Resins.

[2] Park S., Kim J., Woo Han T., Yeon Hwang D., Lee H., Kim W., 2022. Mechanical Reinforcement of UV-Curable Polymer Nanocomposite for Nanopatterned Mold.

[3] Işın D., Kayaman-Apohan N., Güngör A., 2009. Preparation and Characterization of UV-Curable Epoxy/Silica Nanocomposite Coatings.

[4] Li Y., Zhong J., Wu L., Weng Z., Zheng L., Peng S., Zhang X., 2019.High Performance POSS Filled Nanocomposites Prepared via UV-Curing Based on 3D Stereolithography Printing.

[5] Kaynar S., 2016, Effects of Polyhedral Oligomeric Silsesquioxane Reinforced Polypropylene (PP) Nanocomposites on the Thermal, Mechanical, and Optical Properties of PP.

[6] Çiçek B., Aydoğmuş T., Sun Y., 2021. Reçine 3D Yazıcı Ürünlerinin Biyo-Uyumluluk İncelemesi. 67-72

ABSTRACT PRESANTATION/ ÖZET SUNUMLAR

Reaction-Time-Dependent on Synthesis of Graphene Oxide from Waste Tire

Azra Umairah Anuar[a], Noor Najmi Bonnia[a],*, Norashirene Mohamad Jamil[a] , Nor Dalila Nor Affandib

[a]Faculty of Applied Science, Universiti Teknologi MARA, 40450 Shah Alam, Selangor, Malaysia.

(ORCID: 0000-0003-3181-064X), azraumairah99@gmail.com

(ORCID: 0000-0001-9550-8445), noornajmi@uitm.edu.my

(ORCID: 0000-0001-6224-7058), norashirene@uitm.edu.my

[b]Textile Research Group, Faculty of Applied Sciences, Universiti Teknologi MARA, 40450 Shah Alam, Selangor, Malaysia.

(ORCID: 0000-0003-2739-6570), dalila@uitm.edu.my

Abstract

Graphene oxide (GO) has been widely utilized in diverse applications due to its unique properties and versatile functionalization capabilities. Maintaining the optimal synthesis parameters is crucial to producing high-quality GO with high oxidation. This study focuses on the effect of different reaction times during the modified Hummers method on the structural and morphological properties of GO derived from regenerated carbon black (CB) of waste tire. Using reaction times of 60, 120, and 180 minutes, the resulting GO samples were systematically examined through various characterization techniques. FTIR spectroscopy confirmed the increased intensity of O-H bonds vibrations, correlating with longer reaction times. XRD analysis revealed that increasing reaction times resulted in broader and more amorphous peaks, indicative of greater intercalation of oxygen-containing groups. Notably, as the reaction time increase, the oxygen content in the GO also increases, as evidenced by the intensified EDX peaks. Our finding demonstrate that the reaction time significantly influence the degree of oxidation and the distribution of functional groups in GO. This research provides valuable insights into the synthesis of GO from sustainable sources, promoting cost-effective and environmentally friendly approaches to advance the material production.

Keywords: Graphene Oxide; Waste; Tire; Carbon Black.

SPALATOCRETE – BIO-COMPOSITE MADE WITH SPANISH BROOM

Sandra JURADIN[1], Marijo FRANIĆ[2]

[1]University of Split Faculty of Civil Engineering, Architecture and Geodesy, Matice hrvatske 15, Split, Croatia, e-mail: sandra.juradin@gradst.hr
[2]e-mail: mario.franic@gmail.com

Abstract

The construction sector is increasingly examining the possibility of using environmentally friendly building materials. Composite materials are a combination of matrix and particles of different sizes and origins. In ordinary, normal concrete, the matrix is cement stone and the particles are grains of stone aggregate. Replacing cement with some other more environmentally friendly binders and stone aggregate with plant-based biomaterials results in an environmentally friendly material. Such a bio-composite reduces the use of natural resources and waste, which is an important step towards sustainable development in the building materials' industry.

The idea for creating this new composite comes from plant-based biomaterials like hemp, bamboo, flax, etc. Spanish Broom-based concrete named Spalatocrete is composed of Spanish Broom and lime. Spanish Broom (Spartium junceum) is a wild, bushy plant widespread in the Mediterranean area. Until now, the quality of the fibers of this plant has mainly been studied in the textile industry, but recently there are studies in which Spanish broom is considered a reinforcement of composites such as biopolymer, cement mortar and concrete. After separating the fibers, the woody part of the plant remains, which is used as an aggregate in the bio-composite. Several test specimens were made in order to find the most favorable combination of materials. The paper is based on the presentation of the idea of this material, and the tests of material characteristics are the subject of some future research.

By integrating Spanish broom shive and lime into sustainable building practices, this bio-composite presents a promising solution for reducing energy consumption in buildings and minimizing the ecological footprint of construction. The findings of this research indicate that Spanish broom offers not only a sustainable alternative to traditional materials but also a viable contribution to circular economy models and climate change mitigation strategies.

Keywords: bio-composite, Spanish Broom, density, bio-insulation, thermal, acoustic

PHOTOTHERMAL ANTIBACTERIAL ACTIVITY OF PANI/FLY ASH COMPOSITE

Duygu YANARDAĞ KOLA[1], Abdurrahman MUSTAFA[2], Ahmed ALSARORI[3], Gülcihan GÜZEL KAYA[4]

[1]Res. Asst., Konya Technical University, dyanardag@ktun.edu.tr
[2]MSc. Student, Konya Technical University, abdalrahman.mustafa7@gmail.com
[3]MSc. Student, Konya Technical University, alsarori@gmail.com
[4]Assoc. Prof., Konya Teknik University, ggkaya@ktun.edu.tr

Abstract

In this study, photothermal antibacterial activity of polyaniline (PANI)/fly ash composite was investigated against *Staphylococcus aureus (S. aureus)*. PANI/fly ash composite was synthesized by chemical oxidative polymerization method and ammonium persulfate (APS) was used as oxidizing agent in the synthesis. PANI, one of the best-known conducting polymers, has outstanding potential applications for biological applications due to its hydrophilic nature, low toxicity, high electrical conductivity resulting from its good environmental stability, and biocompatibility. The structural properties of the PANI/fly ash composite were studied by FTIR (Fourier Transform Infrared Spectroscopy) and FE-SEM (Field Emission Scanning Electron Microscopy) analysis. In the FTIR analysis, characteristic bands specific to PANI were observed and it was confirmed that a successful composite was formed with fly ash. FE-SEM images were used to study the surface morphology of the composite.

Antibacterial activity of the composite with different material concentrations was determined by the spread plate method. No antibacterial activity was observed against *S. aureus* without NIR irradiation. Fortunately, under 2.5 W cm^{-2} NIR irradiation for 10 min, high antibacterial activity (approximately 99%) was achieved using 100 µg mL^{-1} PANI/fly ash in phosphate buffer solution (PBS). The temperature increases in the case of NIR irradiation provided destruction of the bacteria leading to an effective antibacterial activity. The results show that PANI/fly ash composite can be used in many biomedical applications, especially disinfection.

Keywords: Fly ash; PANI; Photothermal antibacterial activity

INVESTIGATION OF RESISTIVE SWITCHING PROPERTIES OF TRANSITION METAL OXIDE-BASED NANOSTRUCTURE FOR FLEXIBLE ELECTRONICS

Adiba ADIBA[1*], Tufail AHMAD[2]

[1]Department of Physics, Aligarh Muslim University, India adibaeshaal@gmail.com [2]Department of Physics, Aligarh Muslim University, India tufailahmadamu@gmail.com

Abstract

With the growing demand for enhanced computing power and data storage, there is a significant drive to develop high-density, non-volatile memory devices promising high speed, power efficiency, and compatibility with conventional CMOS technology. Resistive switching random-access memory (ReRAM), having a simple metal-insulator-metal (MIM) structure, has emerged as a strong candidate for next-generation memory solutions. Offering advantages like rapid switching, low power consumption, high scalability, and non-destructive readout, ReRAM holds promise for applications in fields such as neuromorphic computing, artificial intelligence, and secure data storage. The resistive switching (RS) effect in ReRAM relies on creating and rupturing conductive filaments (CF) within the insulator layer under applied voltage, allowing the device to toggle between high-resistance and low-resistance states (HRS and LRS). Based on switching, ReRAM devices can be broadly categorized into unipolar RS, Bipolar RS and threshold RS. Materials like transition metal oxides (TMOs), two-dimensional materials, organic materials, and chalcogenides have been extensively studied for the insulating layer due to their reliable RS properties and favorable characteristics such as uniform switching and low energy consumption. Research efforts focus on optimizing device stability, retention, and endurance by techniques like elemental doping, bilayer structures, and nanoparticle integration. These enhancements aim to reduce variability, enable forming-free operation, and improve overall device reliability, making ReRAM a promising pathway toward advanced data storage and bio-inspired neuromorphic computing systems. ReRAM devices are highly adaptable to flexible, wearable, and even stretchable electronics due to their inherent properties and simple structures. Unlike traditional semiconductor memories, ReRAM can maintain performance under physical stress, such as bending or stretching, by using flexible substrates like PET or polyimide, which makes them suitable for applications in next-gen wearable devices or implantable electronics.

Keywords: ReRAM, Resistive Switching, Flexible electronics

The influence of sinusoidal milling on surface quality of CFRP

Sezer Morkavuk*, Uğur Köklü, Fatih Aktaş

*Department of Mechanical Engineering, Karamanoglu Mehmetbey University, Karaman, Turkey

Abstract

Carbon fiber reinforced plastic (CFRP) composites are used in many industries especially in aerospace, marine, and automotive. Although fiber-reinforced composites are produced close to net shape using methods such as vacuum bagging or vacuum-assisted resin transfer molding, machining is inevitable to give the part its final shape. In this study, the influence of sinusoidal milling strategy on cutting forces of CFRP was investigated experimentally. The results showed that sinusoidal milling significantly reduced the cutting forces in X and Y direction and therefore resultant cutting force, while it improved surface quality and reduced damage formation. However, this machining strategy leaves uncut fibers at the end of the workpiece material, which may require a second cutting operation

28.11.2024

ISBN: 978-625-95311-6-8